AD-A191 606 REPAIR EVALUATION MAINTENANCE AND REHABILITATION RESEARCH PROGRAM APPLICA.. (U) GEORGIA INST OF TECH ATLANTA SCHOOL OF CIVIL ENGINEERING R D BARKSDALE 1/1

UNCLASSIFIED DEC 87 WES/TR/GL-REMR-GT-7 DACW39-85-M-2350 F/G 13/13 NL

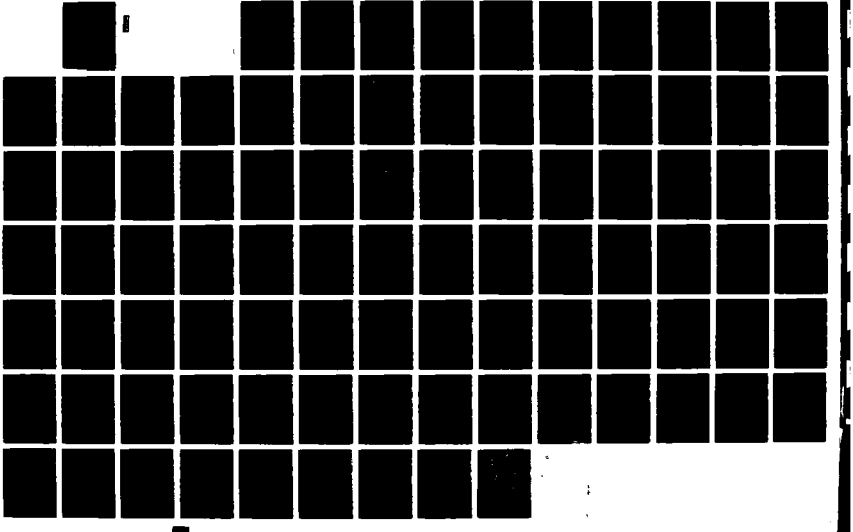

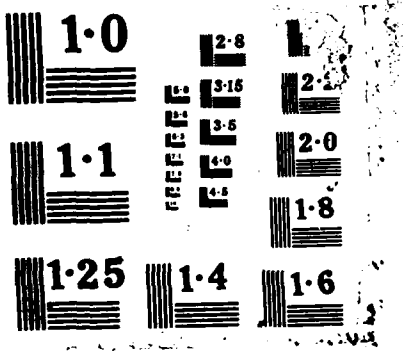
1·0
1·1
1·25
1·4
1·6
1·8
2·0
2·2
2·8
3·15
3·5
4·0
4·5

Unclassified
SECURITY CLASSIFICATION OF THIS PAGE

REPORT DOCUMENTATION PAGE

Form Approved OMB No. 0704-0188

1a. REPORT SECURITY CLASSIFICATION: Unclassified	1b. RESTRICTIVE MARKINGS
2a. SECURITY CLASSIFICATION AUTHORITY	3. DISTRIBUTION / AVAILABILITY OF REPORT: Approved for public release; distribution unlimited.
2b. DECLASSIFICATION / DOWNGRADING SCHEDULE	
4. PERFORMING ORGANIZATION REPORT NUMBER(S)	5. MONITORING ORGANIZATION REPORT NUMBER(S): Technical Report REMR-GT-7
6a. NAME OF PERFORMING ORGANIZATION: School of Civil Engineering, Georgia Institute of Technology; 6b. OFFICE SYMBOL (If applicable)	7a. NAME OF MONITORING ORGANIZATION: USAEWES, Geotechnical Laboratory
6c. ADDRESS (City, State, and ZIP Code): Atlanta, GA 30332	7b. ADDRESS (City, State, and ZIP Code): PO Box 631, Vicksburg, Ms 39180-0631
8a. NAME OF FUNDING / SPONSORING ORGANIZATION: US Army Corps of Engineers; 8b. OFFICE SYMBOL (If applicable)	9. PROCUREMENT INSTRUMENT IDENTIFICATION NUMBER: DACW39-85-M-2358
8c. ADDRESS (City, State, and ZIP Code): Washington, DC 20314-1000	10. SOURCE OF FUNDING NUMBERS: PROGRAM ELEMENT NO. / PROJECT NO. / TASK NO. / WORK UNIT ACCESSION NO. 32275

11. TITLE (Include Security Classification)
Applications of the State of the Art of Stone Columns--Liquefaction, Local Bearing Failures, and Example Calculations

12. PERSONAL AUTHOR(S)
Barksdale, Richard D.

13a. TYPE OF REPORT	13b. TIME COVERED	14. DATE OF REPORT (Year, Month, Day)	15. PAGE COUNT
Final report	FROM _____ TO _____	December 1987	90

16. SUPPLEMENTARY NOTATION
A report of the Geotechnical problem area of the Repair, Evaluation, Maintenance, and Rehabilitation (REMR) Research Program. Available from National Technical Information Service, 5285 Port Royal Road, Springfield, VA 22161.

17. COSATI CODES		
FIELD	GROUP	SUB-GROUP

18. SUBJECT TERMS (Continue on reverse if necessary and identify by block number)
Bearing capacity, Liquefaction, Pore-water pressure, Earthquake loading, In-situ deep compaction,
(Continued)

19. ABSTRACT (Continue on reverse if necessary and identify by block number)

Stone columns offer one potential technique for rehabilitating the foundations beneath existing structures to withstand both static and earthquake loadings. A detailed discussion of stone columns has been given in a previously published Federal Highway Administration (FHWA) report entitled "Design and Construction of Stone Column, Vol I." The present report supplements the FHWA report, presenting earthquake engineering and excess pore pressure considerations and giving the previously unpublished appendixes.

Seed and Booker's method is presented for estimating the dissipation of excess pore pressure in stone column improved ground during strong motion earthquakes.

(Continued)

20. DISTRIBUTION / AVAILABILITY OF ABSTRACT	21. ABSTRACT SECURITY CLASSIFICATION
☒ UNCLASSIFIED/UNLIMITED ☐ SAME AS RPT ☐ DTIC USERS	Unclassified
22a. NAME OF RESPONSIBLE INDIVIDUAL	22b. TELEPHONE (Include Area Code) / 22c. OFFICE SYMBOL

DD Form 1473, JUN 86 Previous editions are obsolete. SECURITY CLASSIFICATION OF THIS PAGE

Unclassified

18. SUBJECT TERMS (Continued).

Remedial treatments
Settlement
Soil reinforcement
Soils
Stability
Stone columns

19. ABSTRACT (Continued).

Practical aspects are discussed of the effects of radial drainage of various techniques of constructing stone columns. The capacity for radial drainage may be reduced during construction because of both smear effects and a change in stone column gradation.

A theory is given for local bearing failure of an isolated stone column subjected to a shear load. Also, a number of examples are presented illustrating the solution of bearing capacity, settlement, slope stability, and liquefaction problems for ground that has been improved with stone columns.

PREFACE

The purpose of this report is to give example calculations and considerations that may be used in the state-of-the-art application of stone columns for improving soils subject to static, earthquake, and post earthquake-reduced strength loading conditions beneath and adjacent to existing structures. This report presents excess pore pressure considerations and the directly pertinent but previously unpublished appendixes to the following report published by the Federal Highway Administration (FHWA): Design and Construction of Stone Columns, Vol I, FHWA, Report No. FHWA/RD-83/026, Final Report, December 1983, 210 pp (by R. D. Barksdale and R. C. Bachus). The appendixes to this report were to be published by the FHWA as Vol II, but budget limitations have prevented their publication; they are given in the present report as Appendixes A through E.

The FHWA Stone Column report considers only briefly liquefaction of sands due to strong motion earthquakes as influenced by stone column construction. Therefore, a method is presented for estimating the dissipation of excess pore pressures due to radial drainage, and practical construction aspects of drainage are considered.

This report was prepared under Contract No. DACW39-85-M-2358 with the US Army Engineer Waterways Experiment Station (WES) during the period July 1985 to December 1986. The investigation was conducted under the Repair, Evaluation, Maintenance, and Rehabilitation (REMR) Research Program Work Unit 32275, "Remedial Improvement for Liquefiable Foundations." Mr. Arthur H. Walz, Headquarters, US Army Corps of Engineers (HQUSACE), was Technical Monitor for HQUSACE for this work.

The REMR Overview Committee, which approved this study, consisted of Mr. John R. Mikel (DAEN-CWO-M), Mr. Bruce L. McCartney (DAEN-CWH-D), and Dr. Tony C. Liu (DAEN-ECE-D). Coordinator for the Directorate of Research and Development was Mr. Jesse A. Pfeiffer, Jr. (DAEN-RDC), and the REMR Program Manager was Mr. William F. McCleese, Concrete Technology Division, Structures Laboratory, WES.

Mr. Richard H. Ledbetter, Earthquake Engineering and Geophysics Division (EEGD), Geotechnical Laboratory (GL), was Technical Monitor for the WES, under the supervision of Dr. Arley G. Franklin, Chief, EEGD, and under the general supervision of Dr. William F. Marcuson III, Chief, GL. Appreciation

is extended for Mr. Ledbetter's help and careful review of the manuscript. Special thanks also go to Dr. P. F. Hadala, Assistant Chief, GL, for his thorough review of the manuscript. Appreciation is expressed to the Federal Highway Administration for granting special permission to allow the publication of the appendixes to the stone column report. Mr. A. F. DiMillio was Project Manager, and Mr. Jerry DiMaggio was Technical Monitor for the Federal Highway Administration.

COL Dwayne G. Lee, CE, was the Commander and Director during the publication of this report. Dr. Robert W. Whalin was Technical Director.

CONTENTS

	Page
PREFACE	1
CONVERSION FACTORS, NON-SI TO SI (METRIC) UNITS OF MEASUREMENT	4
PART I: INTRODUCTION	5
Stone Column Soil Improvement Mechanisms--Earthquake Loading	7
Summary	9
PART II: RADIAL DISSIPATION OF EXCESS PORE PRESSURES DEVELOPED DURING EARTHQUAKES	11
Introduction	11
Liquefaction Design Charts Considering Radial Drainage	11
Drain Permeability	17
PART III: SUMMARY AND CONCLUSIONS	22
REFERENCES	24
APPENDIX A: SELECTED CONTACTS FOR STONE COLUMNS	A1
APPENDIX B: LOCAL BEARING FAILURE OF AN ISOLATED STONE COLUMN	B1
Local Bearing Failure	B3
Lateral Bearing Failure in Cohesive Soil	B4
Calculation of Limiting Shear Force	B6
Design Charts	B7
Design	B13
APPENDIX C: EXAMPLE BEARING CAPACITY PROBLEMS	C1
Bearing Capacity Example 1	C1
Bearing Capacity Example 2	C5
APPENDIX D: EXAMPLE SETTLEMENT PROBLEMS	D1
Settlement Example 1	D1
Settlement Example 2	D9
APPENDIX E: EXAMPLE STABILITY PROBLEM	E1
APPENDIX F: EXAMPLE PROBLEM OF PORE PRESSURE DISSIPATION DURING AN EARTHQUAKE	F1
APPENDIX G: NOTATION	G1

CONVERSION FACTORS, NON-SI TO SI (METRIC)
UNITS OF MEASUREMENT

Non-SI units of measurement used in this report can be converted to SI (metric) units as follows:

Multiply	By	To Obtain
feet	0.3048	metres
horsepower (550 foot-pounds (force) per second)	745.6999	watts
inches	2.54	centimetres
kips (force)	4.448222	kilonewtons
kips (force) per square foot	47.88026	kilopascals
kips (mass) per cubic foot	16018.46	kilograms per cubic foot
pounds (force) per square foot	47.88026	pascals
pounds (force) per square inch	6.894757	kilopascals
pounds (mass)	0.4535924	kilograms
pounds (mass) per cubic foot	16.01846	kilograms per cubic metre
square feet	0.09290304	square metres
tons (2,000 pounds, mass)	907.1847	kilograms

APPLICATIONS OF THE STATE OF THE ART OF STONE COLUMNS--LIQUEFACTION, LOCAL BEARING FAILURE, AND EXAMPLE CALCULATIONS

PART I: INTRODUCTION

1. Stone columns offer one method of rehabilitating existing structures to withstand both static and earthquake loadings. They can also be placed adjacent to structures both above and below the water surface. Special techniques are available for constructing stone columns (or sand compaction piles) below water (Barksdale and Dobson 1983, Barksdale 1987, Aboshi et al. 1979). Stone columns can be used, with careful consideration of seepage conditions, beneath existing embankments and dams. Although they can be installed through existing dams, there is a real question of whether or not they should be.

2. Construction of stone columns within an earth dam can increase pore pressures below the dam particularly near the upstream face when the embankment is impervious, or when an impervious layer of clay underlies the dam. On the downstream side of the dam, flow is concentrated at the stone columns which would act as drains. Seepage erosion could take place at this location of finer particles into the stone column drain under, for example, steady state seepage conditions. This condition of seepage erosion would be further aggravated in regions where flow to the stone column is even further concentrated, such as in a pervious layer near its contact with an impervious layer. These important aspects which have a direct impact on dam safety certainly deserve careful consideration and further study.

3. For many site and loading conditions, stone columns offer an excellent alternative to prevent liquefaction and to improve stability and bearing capacity of weak soils. They also significantly increase the rate at which consolidation settlement occurs. Stone columns decrease the magnitude of settlement, with the maximum amount of improvement being about 50 percent settlement reduction for soft cohesive soils if about 35 percent of the soil is replaced by stone.

4. For both static and earthquake loadings, stone columns can be used to improve soft to firm clays, silty sands, and sands having silt and clay layers. Stone columns can be constructed using either wet or dry processes.

Usually, a coarse stone having a variation in grain size from 0.5-in.* up to 2- to 3-in. maximum size is used in the wet process. A comprehensive description of the design, construction, and general utilization of stone columns has been given by Barksdale and Bachus (1983) and by Barksdale and Dobson (1983). A general summary comparison including advantages and disadvantages of available construction techniques for granular columns has been given by Barksdale (1987).

5. The purpose of this report is to give example calculations and considerations that may be used in the state-of-the-art application of stone columns for improving soils subject to static, earthquake, and post-earthquake-reduced strength loading conditions beneath and adjacent to existing structures. This report presents excess pore pressure considerations and the previously unpublished appendixes to the report entitled "Design and Construction of Stone Columns, Vol. I," published by the Federal Highway Administration (FHWA) (Barksdale and Bachus 1983). These appendixes are directly pertinent to the application of stone columns for remedial treatment of liquefiable soils.

6. Appendixes A through E of this report presents the material in the same order as referred to in the FHWA report. Appendix A gives addresses of contractors and engineers involved with stone column construction. It is not an all inclusive list of such organizations and individuals. For the United States, the listing includes the contractors currently capable of constructing stone columns, and for Europe and Asia, the major contractors that have the capability. Appendix B describes a theory for estimating local bearing failure of a single stone column (or sand compaction pile) subjected to a shear loading. Appendixes C, D, and E give example problems illustrating the use of stone columns for bearing capacity, settlement, and stability problems, respectively.

7. Appendixes B through E are intended to be used in conjunction with the corresponding theory, equations, figures, and tables presented in the original FHWA report by Barksdale and Bachus (1983). Sections of the FHWA report that present the theory associated with Appendixes B through D of this report are given in Table 1 as a convenient cross-reference guide.

---

* A table of factors for converting non-SI units of measurement to SI (metric) units is presented on page 4.

Table 1

Cross-Reference Between Appendixes of This Report and Theory Presented in FHWA Report "Design and Construction of Stone Columns"

Appendix	Topic	Reference Sections of FHWA Report (Barksdale and Bachus 1983)
B	Local Bearing Failure	Chapter VII, pp. 153-163
C	Bearing Capacity	Theory: Chapter III, pp. 38-46 Design: Chapter VII, pp. 142-145
D	Settlement Analysis	Theory: Chapter III, pp. 47-76 Design: Chapter VII, pp. 145-152
E	Stability	Theory: Chapter III, pp. 76-84 Design: Chapter VII, pp. 152-165
F	Pore Pressure	Smear: Chapter III, pp. 73-74 Chapter IV, pp. 100-105 Chapter VII, pp. 150-151 Construction Methods: Chapter II

Note: The basic theory given in Chapter III, pp. 27-38, of the FHWA report is applicable to Appendixes B through E.

8. In addition, the present report considers the important concept of the dissipation of earthquake generated excess pore pressures due to radial drainage into stone columns (or stone drains). The theoretical approach developed by Seed and Booker (1976) for evaluating excess pore pressure dissipation is summarized, and a design example is given in Appendix F. Although pore pressure dissipation concepts are presented in the present report, Table 1 gives a cross-reference to appropriate sections of the FHWA report describing smear, which is a very important factor in radial drainage.

Stone Column Soil Improvement Mechanisms--Earthquake Loading

9. Construction of stone columns can under certain conditions improve the ground when subjected to a strong motion earthquake due to (a) densification of in situ granular soils surrounding the stone column, (b) the shear strength contributed by the stone columns, and (c) the dissipation of excess pore pressures through radial drainage to the stone columns. The concepts involved with these three mechanisms of improvement are briefly summarized in this section.

Densification

10. The heavy vibrator used to install stone columns densifies clean sands and to a lesser extent dirty sands. Some benefit is even derived from installing stone columns in sandy silts, silts, and clays although the improvement may take several months to become apparent, and is usually not relied upon in design because of the lack of knowledge concerning lateral stress behavior and strength gain with time.

11. If a heavy vibrator is used having 150 hp or more, the soil is subjected to a relatively severe condition of vibration during stone column construction. This vibration level is probably equivalent to a moderate to severe earthquake.

12. The relative density of sands achieved when stone columns are constructed in the field is dependent upon several factors: (a) size (horsepower) and type vibrator, (b) stone column spacing, and (c) characteristics of the in situ soil including fines content, grain size, and gradation. The type fines (i.e., amount of silt compared to the amount of clay) also influences performance. For usual stone column construction equipment and spacings of about 6 to 9 ft, relative densities of 70 to 85 percent can be usually achieved in sands having fines contents less than about 5 percent. Figure 1 gives a generalized relationship between relative density and sand characteristics. This relationship can be used as a preliminary guide in design.

Shear strength of stone column

13. Stone columns typically replace about 20 to 35 percent of the soil being improved. Also, the coarse, open-graded stone used in constructing the stone column is quite dense and not likely to undergo liquefaction. Therefore, the shear strength of the stone column can contribute a significant amount of lateral force resistance during an earthquake. Shear strength of the stone column was, for example, relied upon at the Santa Barbara sewerage treatment plant (Engelhardt and Golding 1975, Mitchell and Huber 1985, Barksdale and Bachus 1983) to carry the design earthquake loading.

14. To be able to rely upon the stone column for shear strength during an earthquake, some degree of lateral support must be present around the column. Field shear tests are an excellent approach for evaluating the resistance of the stone column and/or the composite soil mass. Also, in very soft soils consideration should be given to the possibility of local bearing failure (Appendix B).

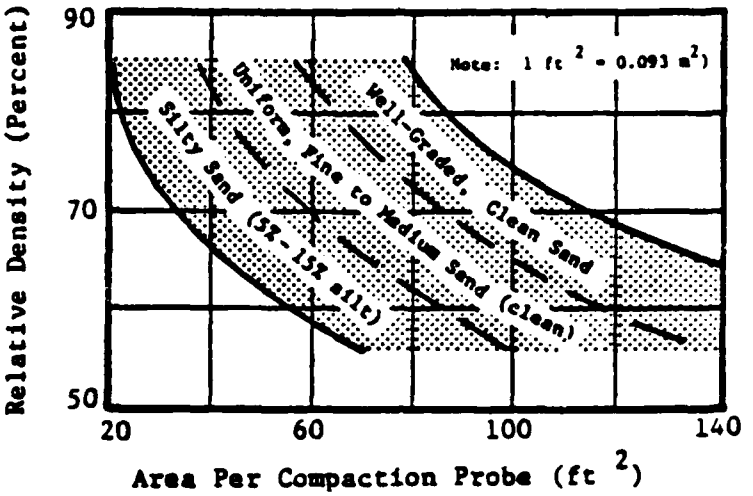

Figure 1. Approximate variation of relative density with tributary area--for preliminary design only (Barksdale and Bachus 1983)

Pore pressure dissipation

15. If the excess pore pressures generated during an earthquake are dissipated quickly enough, liquefaction will not occur. The construction of stone columns on relatively close centers provides vertical drains which greatly reduce the radial flow path and, if properly constructed, can be quite effective in dissipating excess pore pressures. Part II of this report considers in detail the radial dissipation of excess pore pressures generated during an earthquake.

Summary

16. In design frequently just one of the mechanisms of stone column improvement discussed in paragraphs 8 through 14 is considered to resist earthquake effects. In the past, for example, only the shear strength due to the stone column has frequently been used in design. In actuality, two or even all three of these mechanisms will probably actively contribute to the stability of the soil mass when subjected to seismic loadings. The relative contribution of each mechanism depends upon many factors: (a) construction technique used, (b) specific site conditions, and (c) characteristics of the design earthquake. Having several different mechanisms of defense against failure is in many instances an important advantage over other alternative approaches

which may rely on a single mechanism. Finally, caution should be exercised in using stone columns having a coarse gradation in water resource applications where steady state or transient seepage conditions exist.

PART II: RADIAL DISSIPATION OF EXCESS PORE PRESSURES DEVELOPED DURING EARTHQUAKES

Introduction

17. Methods for predicting the buildup of excess pore pressures in sand due to earthquakes have been summarized for example by Seed (1976) and Finn (1984). Seed, Martin, and Lysmer (1976) concluded that in homogeneous coarse sands (D_{20} > 0.7 mm), the pore pressures generated by an earthquake may be dissipated because of vertical drainage as quickly as they develop. In typical alluvial deposits, however, numerous clay and silt layers which will prevent vertical drainage are likely to be present. Installation of relatively closely spaced stone columns (or stone drains) composed of an open-graded stone results in radial drainage (Figure 2), which is not significantly influenced by soil stratification.

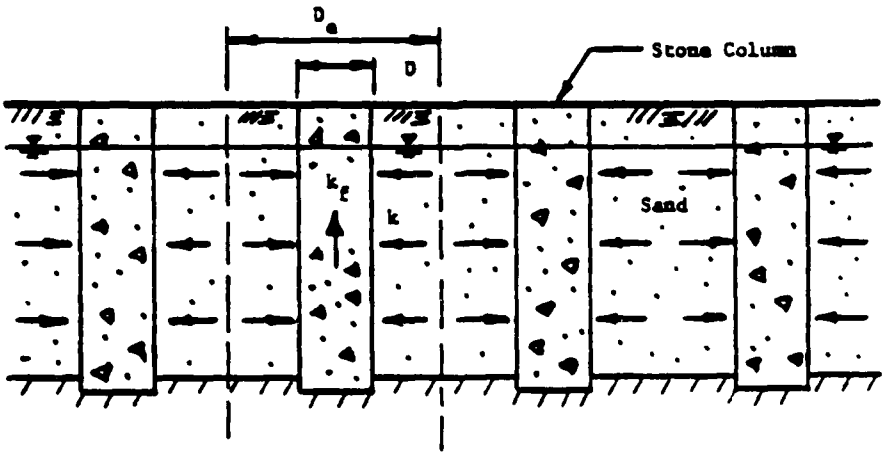

Figure 2. Radial drainage to stone columns

Liquefaction Design Charts Considering Radial Drainage

18. Seed and Booker (1976) have developed easy to use design charts for selecting the required spacing of stone columns (or stone drains) to dissipate earthquake-generated pore pressures in sand layers. The geometry associated with radial drainage to stone columns is shown in Figure 2. As illustrated in

the figure, important geometric variables are the diameter D^* of the constructed stone column and the equivalent diameter D_e of the area tributary to the column. For an equilateral triangular pattern of stone columns, the equivalent diameter of the tributary area is

$$D_e = 1.05s \tag{1}$$

and for a square grid pattern

$$D_e = 1.13s \tag{2}$$

where s is the uniform spacing of stone columns.

19. Now assume that the design earthquake can be represented by a series of N_{eq} uniform cycles of stress having a magnitude τ_{eq} over a period of time t_d. Further, assume the sand layer will liquefy under the earthquake loading τ_{eq} after being subjected for undrained conditions to N_ℓ uniform stress cycles of the design earthquake. Methods for evaluating these design parameters have been described, for example, by Seed (1976) and Seed and Idriss (1982); refer to these references for a complete discussion of how N_{eq}, τ_{eq}, t_d, and N_ℓ can be estimated.

20. During an earthquake the induced excess pore pressures vary with both time and position within the zone tributary to a stone column. Now let u be the induced pore pressure in the sand layer during the earthquake and σ_o the initial effective stress in the layer. The greatest pore pressure ratio $r_g = u/\sigma_o$ in the sand layer during the earthquake can be calculated for conditions of radial drainage using Figures 3 through 6. The average value of pore pressure ratio $\bar{r}_g$ taken over the area tributary to the stone column is given in Figures 7 through 10. To determine either pore pressure ratio, the following dimensionless time factor is used:

$$T_{ad} = \frac{4k_r t_d}{\gamma_w m_{v3} D^2} \tag{3}$$

where

k_r = horizontal permeability of the sand stratum

---

* For convenience, symbols and abbreviations are listed in the Notation (Appendix G).

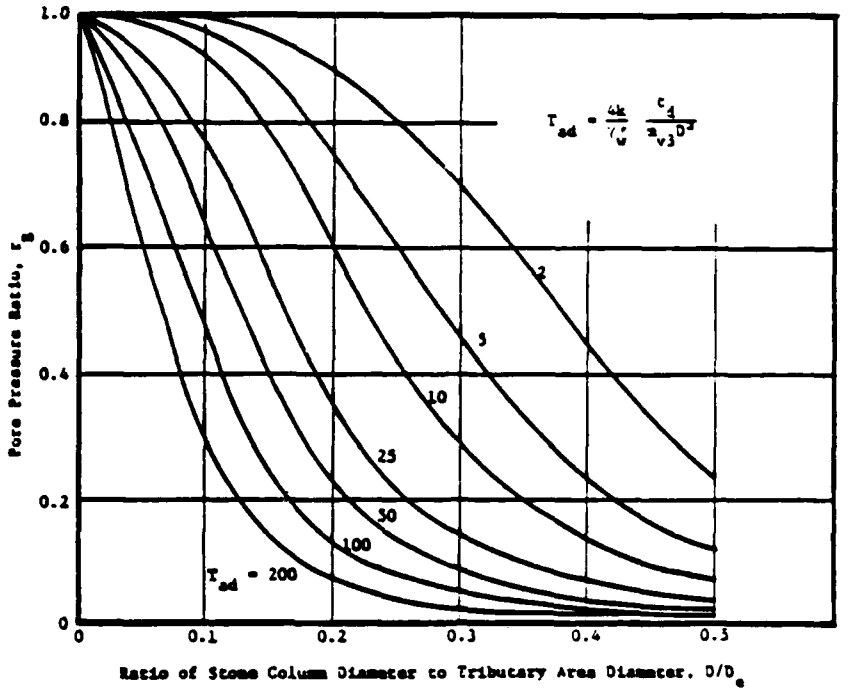

Figure 3. Relationship between greatest pore pressure ratio and drain system parameters for $N_{eq}/N_{\ell} = 1$

(adapted from Seed and and Booker 1976)

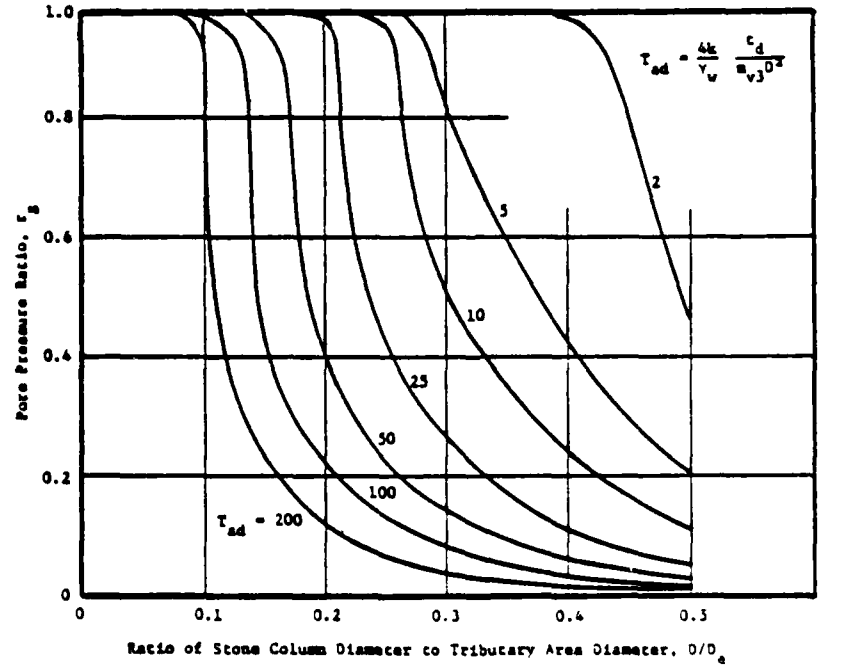

Figure 4. Relationship between greatest pore pressure ratio and drain system parameters for $N_{eq}/N_{\ell} = 2$

(adapted from Seed and Booker 1976)

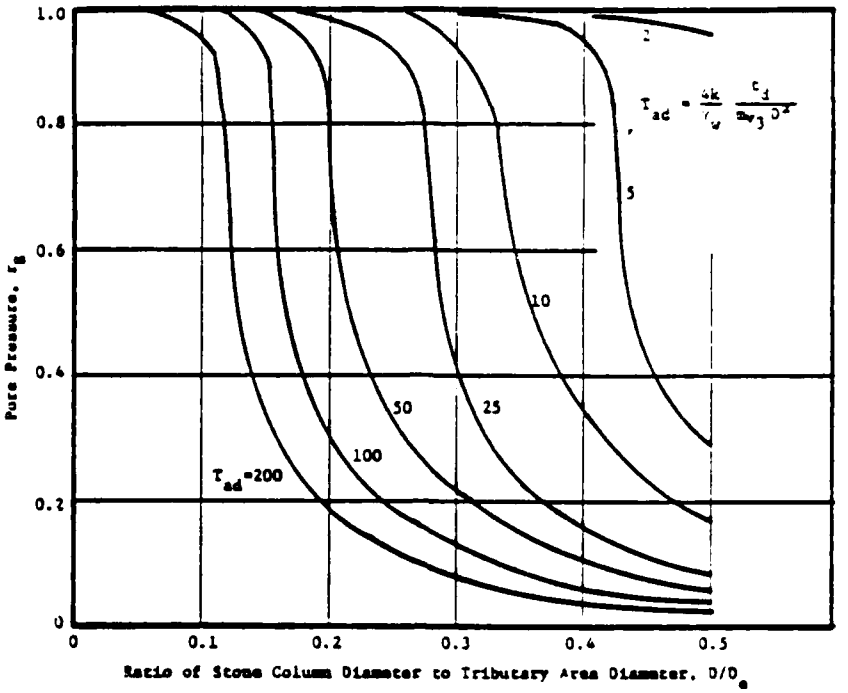

Figure 5. Relationship between greatest pore pressure ratio and drain system parameters for $N_{eq}/N_{\ell} = 3$

(adapted from Seed and Booker 1976)

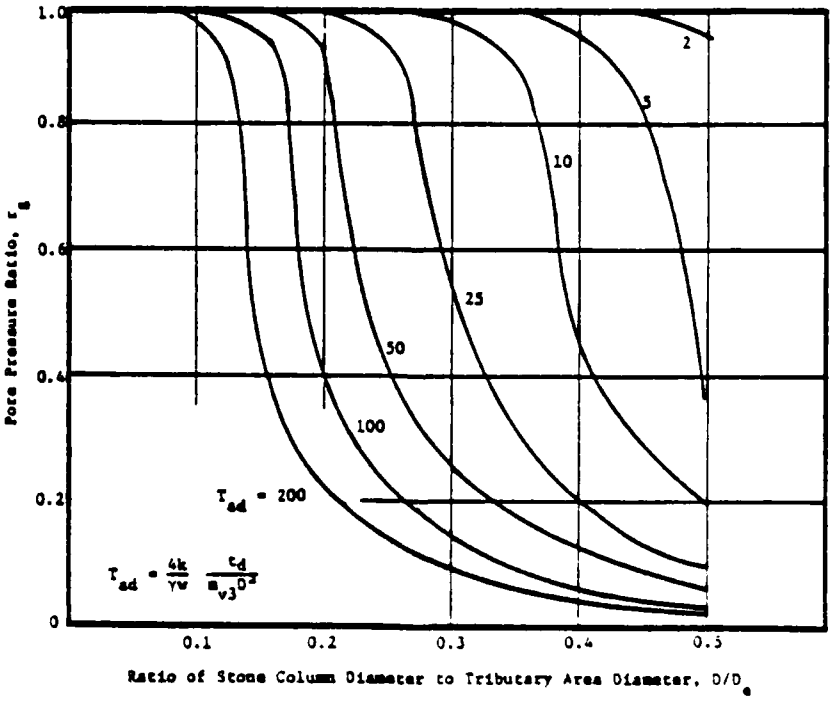

Figure 6. Relationship between greatest pore pressure ratio and drain system parameters for $N_{eq}/N_{\ell} = 4$

(adapted from Seed and Booker 1976)

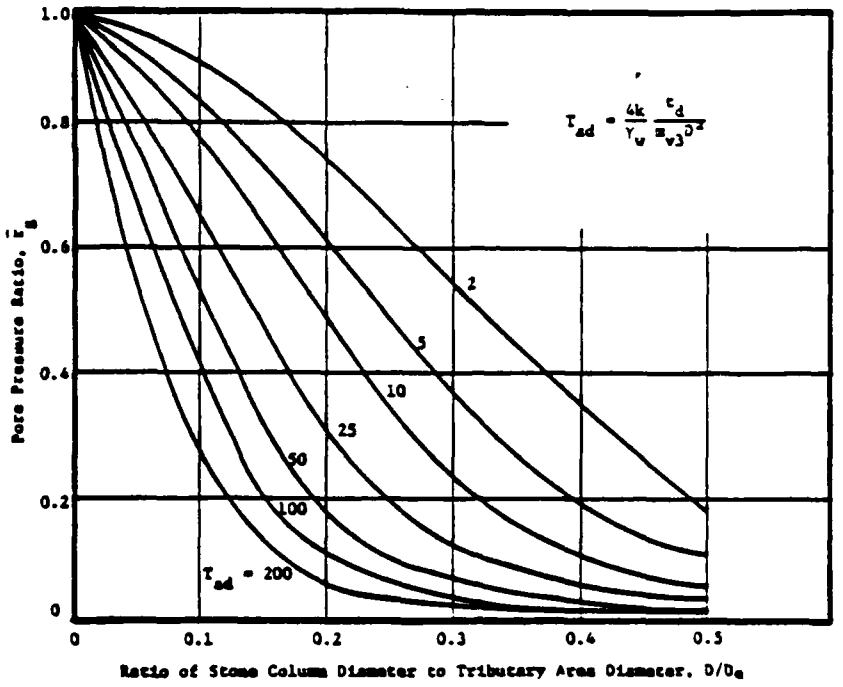

Figure 7. Relationship between greatest average pore pressure ratio and drain system parameters for $N_{eq}/N_\ell = 1$ (adapted from Seed and Booker 1976)

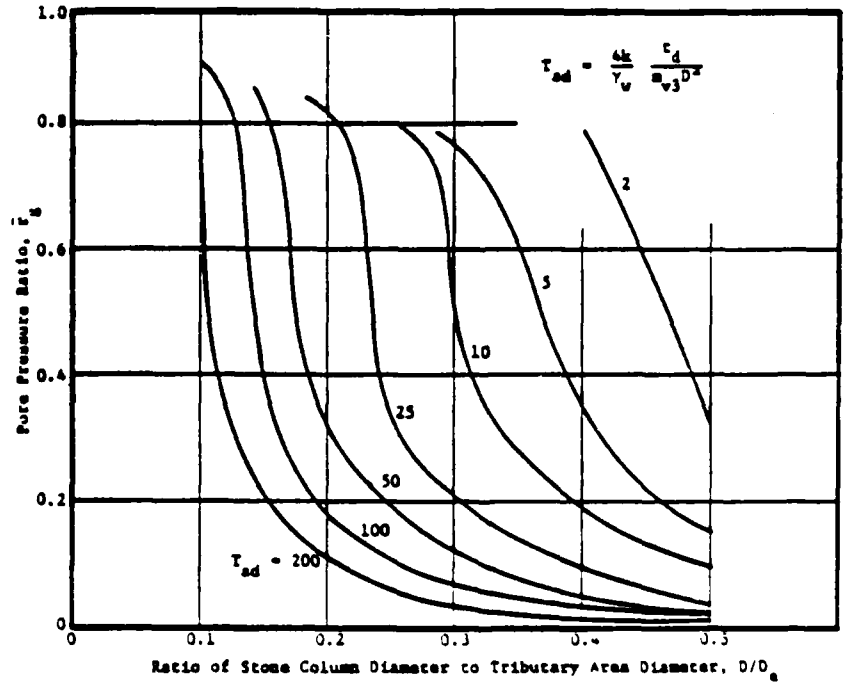

Figure 8. Relationship between greatest average pore pressure ratio and drain system parameters for $N_{eq}/N_\ell = 2$ (adapted from Seed and Booker 1976)

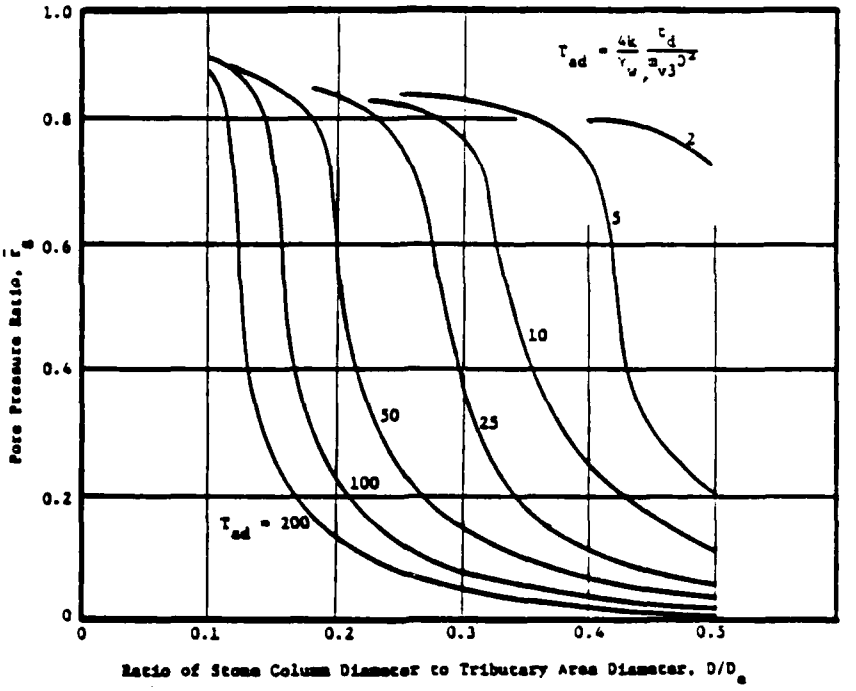

Figure 9. Relationship between greatest average pore pressure ratio and drain system parameters for $N_{eq}/N_{\ell} = 3$ (adapted from Seed and Booker 1976)

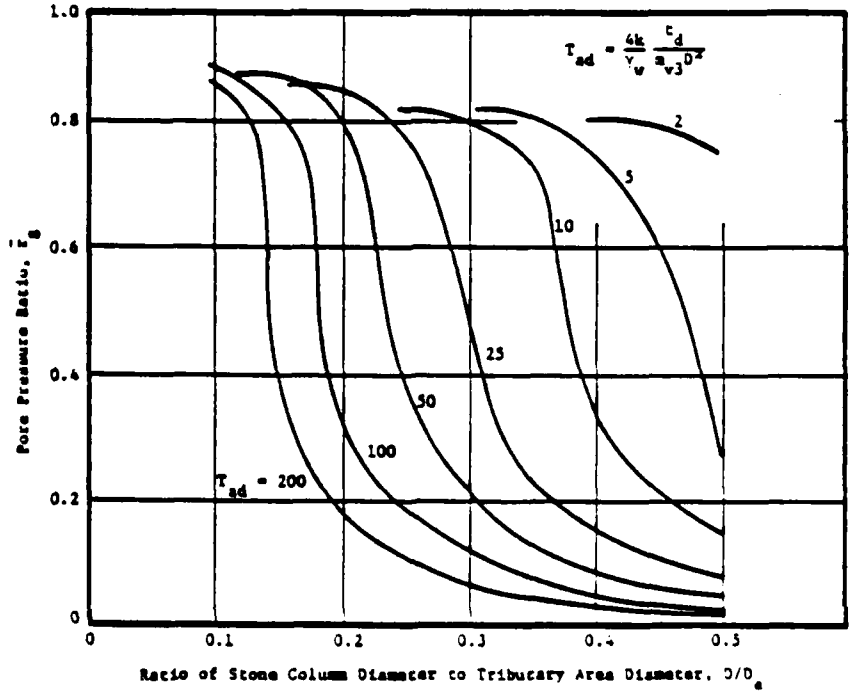

Figure 10. Relationship between greatest average pore pressure ratio and drain system parameters for $N_{eq}/N_{\ell} = 4$ (adapted from Seed and Booker 1976)

t_d = time over which the N_{eq} uniform stress cycles of the earthquake are applied

γ_w = unit weight of water

m_{v3} = coefficient of compressibility

D = diameter of the stone column

The terms in the other ratios used in the figures have been previously defined. Liquefaction in the sand layer would begin to occur when $r_g = 1$, using the relationships in Figures 3 through 6 for the greatest pore pressure ratio. In Figures 7 through 10 similar relationships are given for the average pore pressures developed in the layer. For design a suitable safety factor should be applied to the pore pressure ratio.

21. The theoretical development by Seed and Booker (1976) of the radial drainage theory just presented includes the following assumptions:

a. Vertical drain is infinitely permeable.

b. Darcy's Law is valid.

c. Flow of water occurs in only the radial direction.

d. The radial coefficient of soil permeability is constant.

e. The coefficient of volume compressibility is constant.

f. The change in bulk stress in the sand is negligible.

g. An irregular cyclic earthquake loading can be converted to an equivalent number of uniform stress cycles.

h. The induced pore pressure ratio r_g as a function of the cyclic loading ratio (N_{eq}/N_ℓ) can be approximated using the approach of DeAlba, Chan, and Seed (1975) for an α_1 value of 0.7 (refer to the DeAlba, Chan, and Seed paper for the definition of α_1).

Drain Permeability

22. For the radial pore pressure dissipation theory just discussed to be valid, the stone columns which act as vertical drains must be sufficiently permeable so that a buildup in excess pore pressure does not occur within the column. Seed and Booker (1976) concluded that a drain permeability 200 times greater than the adjacent sand being drained is sufficient to satisfy this requirement. As shown in Figure 11 for a selected earthquake, Seed and Booker's results indicate that important beneficial effects of stone columns may be achieved even if the permeability ratio is as small as 50 to 100. It

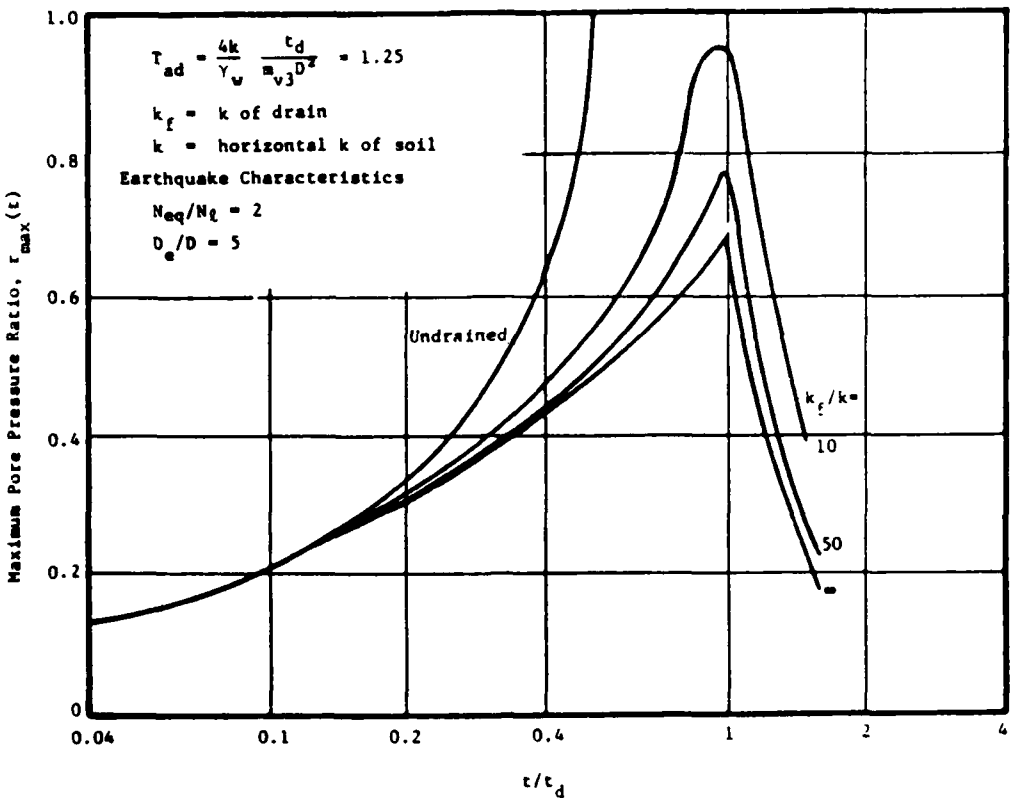

Figure 11. Effect of permeability of stone column backfill on rate of pore pressure dissipation (adapted from Seed and Booker 1976)

is unlikely that a stone gradation can be selected that is both free draining and at the same time satisfies filter criteria developed to prevent erosion of native soil and subsequent clogging of the drain.

23. An important limitation of relying on stone columns for lateral drainage during an earthquake is that local sand may be deposited during construction within the voids of stone columns installed by the conventional vibro-replacement (wet) technique. For example, at Santa Barbara (Barksdale and Bachus 1983) where stone columns were used, 0 to 2 percent of the stone column material passed the 0.5-in. sieve when it was delivered to the site. After construction, however, the amount passing the 0.5-in. sieve had increased to between 11 and 23 percent. Such an increase in sand content has also been informally observed after stone column construction at other sites.

24. Careful consideration must therefore be given during design to the possibility of an important reduction in permeability of the stone column during construction when native sands are present. Further research is needed

to more clearly establish the variation of gradation with depth within the stone column and the extent of reduction in stone column permeability due to deposition of native sand.

Smear effects

25. In constructing stone columns (or other type vertical drains) in cohesive soils, a zone of in situ soil becomes smeared and remolded at the interface between the column and adjacent soil. Also, stone is forced into the soil surrounding the column. These factors all reduce the permeability of a zone around the outside of the stone column and hence can reduce its effectiveness in dissipating excess pore pressures. The combined effects of smear, soil disturbance, and intrusion is generally simply referred to as "smear."

26. A study by Cassagrande and Poulos (1968) has shown that if a casing is advanced without the aid of jetting, the effective horizontal permeability of the soil can be as much as 10 times less due to smear effects than if jetting is used. Hence, use of a method to construct stone columns (or sand compaction piles) which uses jets to aid in advancing the vibroflot (or casing) should cause much less smear especially where cohesive soils are present than a technique which does not employ jets.

Special construction techniques

27. As just discussed, the method of stone column construction used may have an important effect on (a) the gradation of the completed stone column and (b) the amount of smear and hence the effective radial permeability. Two possible techniques that can be used to minimize one or both of these effects are the "pull-down" construction technique (Barksdale and Bachus 1983, Barksdale and Dobson 1983) and the sand compaction pile technique (Barksdale 1987).

28. Both of these methods avoid the potential problem of an important change in gradation of the stone column occurring during construction. If side jets are not used, however, smear along the sides of the column will be increased, particularly where cohesive soils are present.

29. Sand compaction piles. The sand compaction pile method of construction can be used in both sands and soft clays. This technique involves driving a hollow casing (pipe) down to the desired elevation using a vertical vibrator. As the casing is being driven, it is generally filled from the top with a granular material using a special hopper system to handle the sand. A sand is usually used in Japan, although a coarse stone can just as readily be employed.

Indeed, crushed stone and/or gravel have been used in both Japan and Taiwan in this type construction.

30. The sand compaction pile method of construction as presently practiced does not use jets on the sides of the casing. Driving the casing down without the aid of jets would increase the amount of smear occurring in cohesive strata. Smear from cohesive layers may even be dragged down into adjacent cohesionless strata. Therefore, smear in cohesionless layers may become important, particularly where these strata are thin. The use of jets on the sides of the casing may be possible in sand compaction pile construction, which would minimize smear effects.

31. Cased hole stone columns. Special "pull-down" type equipment can also be used to construct stone columns at some sites (Barksdale and Dobson 1983, Barksdale and Bachus 1983). In summary, the pull-down rig uses a standard vibroflot tube for constructing the stone columns. A smaller diameter feeder pipe, however, is attached to the vibroflot. The granular stone column backfill material which may consist of either stone or sand is fed to the bottom of the vibroflot through the smaller feeder tube as the vibroflot is slowly withdrawn from the ground. Although the rig is designed to push the vibroflot and feeder tube down through soft cohesive soils, side jets and the vibrator located at the bottom of the vibroflot can also be used, for example, in sands. Using this equipment, the hole is fully supported throughout construction, and sand can even be used as the backfill material.

32. For site conditions where the pull-down technique can be used, the problem would be eliminated of mixing local in situ sands with the coarse backfill stone placed during stone column construction. A maximum stone size of only about 1.5 in. can, however, be used with present pull-down type rigs. To minimize smear effects, the side jets on the vibroflot should be used throughout construction of the column.

33. Summary. Careful consideration should be given during design of the potential reduction in the effectiveness of drains because of the possibility of deposition of native sand in the stone column and smear effects. The magnitude of these adverse effects depends greatly upon the construction technique used. Extensive field evidence does show that for static load applications, stone columns act as quite effective drains. A similar extensive experience record demonstrating the ability of stone columns to act as drains during strong motion earthquakes has not been developed. Particular

caution should be used where stone columns are employed in and/or beneath water resource structures in which important hydraulic gradients exist over an extended period of time due to either transient or steady state seepage conditions. Installation of stone columns can cause increased pressures and could lead to seepage erosion into the stone column. Essentially no experience has been gained with the use of stone columns under these conditions, and further study is certainly needed.

PART III: SUMMARY AND CONCLUSIONS

34. Design charts are presented for estimating under earthquake loading conditions the radial dissipation to stone columns (or stone drains) of excess pore pressures generated in sand layers. For these charts to be valid the stone columns must have a permeability about 200 times greater than the sand being drained. The construction techniques used to install stone columns can have a signification effect on the resulting permeability of both the stone column and surrounding soil.

35. During design careful consideration should be given to the possibility of a reduction in stone column permeability which may occur using the conventional "wet" vibro-replacement technique. This reduction in permeability can be caused where local sands are present as a result of their deposition during construction into the pores of the coarse stone backfill. Possible alternatives to the conventional wet technique are the pull-down and sand compaction pile techniques which both use a cased hole.

36. The effective lateral permeability of cohesive soils is reduced during stone column construction because of smear. Smear occurs at the interface between the stone column and the surrounding cohesive soil. It can significantly reduce the effective lateral permeability of the cohesive soil caused by remolding and intrusion of soil into the stone. Field studies have shown that the effective lateral permeability of soils adjacent to drains constructed by pushing a pipe in the ground without jetting are about 10 times less than drains constructed using jetting.

37. Where thin layers of sands and clays are present, smear from the cohesive soils may be dragged into the sand layers and hence may also reduce their effective permeability. Further research is needed to better define both smear effects and changes in stone column gradation which occur during construction.

38. For applications where stone columns are subjected to a shear load, a local bearing failure could occur involving punching of the stone column into the surrounding soil. For usual conditions, local bearing failures are most likely to occur in cohesive soils having undrained shear strengths less than about 200 to 400 psf. For soils having lower shear strengths or when an angle of internal friction greater than about 42 deg is used for the stone column, the theory given in Appendix B can be used as a design guide. The

local bearing failure theory presented is for a single, isolated stone column.

39. Several examples are presented illustrating the use of theory to predict the behavior of ground that has been improved using stone columns. Examples of bearing capacity, settlement, stability, and dissipation of excess pore pressures due to earthquakes are presented in Appendixes C, D, E, and F, respectively. Except for the excess pore pressure dissipation theory presented in this report, the theoretical development necessary to solve these problems is given in a previously published report (Barksdale and Bachus 1983). Table 1 of the present report gives a cross-reference between the previously presented theory and the illustrative examples given in the appendixes.

REFERENCES

Aboshi, H., Ichimoto, E., Enoki, M., and Harada, K. 1979. "The Compozer - A Method to Improve Characteristics of Soft Clays by Inclusion of Large Diameter Sand Columns," Proceedings, International Conference on Soil Reinforcement: Reinforced Earth and Other Techniques, Vol I, Paris, pp 211-216.

Barksdale, R. D. 1987. "State-of-the-Art for Design and Construction of Sand Compaction Piles," Technical Report REMR GT-4, US Army Engineer Waterways Experiment Station, Vicksburg, Miss.

Barksdale, R. D., and Bachus, R. C. 1983. "Design and Construction of Stone Columns," Vol I, Federal Highway Administration, Report FHWA/RD-83/026.

Barksdale, R. D., and Dobson, T. 1983. "Improvement of Marginal Urban Sites Using Stone Columns," Proceedings, 34th Annual Highway Geology Symposium and Field Trip, Stone Mountain, Ga., pp 140-156.

Cassagrande, L., and Poulos, S. 1968. "On the Effectiveness of Sand Drains," Canadian Geotechnical Journal, Vol 6, pp 287-326.

DeAlba, P., Chan, C. K., and Seed, H. B. 1975. "Determination of Soil Liquefaction Characteristics by Large-Scale Laboratory Tests," Report EERC 74-14, University of California, Berkeley, Earthquake Engineering Research Center, Berkeley, Calif.

Engelhardt, K., and Golding, H. C. 1975. "Field Testing to Evaluate Stone Column Performance in a Seismic Area," Geotechnique, Vol 25, No. 1, pp 61-69.

Finn, W. D. L. 1984. "Liquefaction Potential: Developments since 1976," International Conference on Case Histories in Geotechnical Engineering, Vol II, St. Louis, Mo. pp 655-681.

Mitchell, J. K., and Huber, T. R. 1985. "Performance of a Stone Column Foundation," Geotechnical Journal, American Society for Civil Engineers, Vol 111, No. GT2, pp 205-223.

Seed, H. B. 1976. "Evaluation of Soil Liquefaction Effects on Level Ground During Earthquakes," Liquefaction Problems in Geotechnical Engineering, American Society for Civil Engineers National Convention, Preprint 1752, Philadelphia, Pa. pp 1-104.

Seed, H. B., and Booker, J. R. 1976. "Stabilization of Potentially Liquefiable Sand Deposits," Report EERC 76-10, University of California, Berkeley, Earthquake Engineering Research Center, Berkeley, Calif.

Seed, H. B., and Idriss, I. M. 1982. "Ground Motions and Soil Liquefaction During Earthquakes," University of California, Berkeley, Earthquake Engineering Research Center, Berkeley, Calif., 134 pp.

Seed, H. B., Martin, P. P., and Lysmer, J. 1976. "Pore Water Pressure Changes During Soil Liquefaction," Geotechnical Journal, American Society for Civil Engineers, Vol 102, No. GT4, pp 323-346.

APPENDIX A: SELECTED CONTACTS FOR STONE COLUMNS

UNITED STATES

Vibroflotation Foundation Company
600 Grant Street
93rd Floor
Pittsburg, Pennsylvania 15219
Phone: 412/288-7676

Mr. George O. H. Reed

GKN Hayward Baker
6820 Benjamin Road
Tampa, Florida 33614
Phone: 813/884-3441

Mr. Tom Dobson
Mr. Mark Koelling

Kencho, Inc.
25030 Viking Street
Hayward, California 94545
(Sand Compaction Piles)
Note: Toyomenka (America), Inc., was formerly the trading company for the Kensetsu Kikai Chosa Co., Ltd. Vibrators. Kencho, Inc., a division of Kensetsu Kikai Chosa Co., Inc., is now selling its own equipment in the United States
Phone: 415/887-3836

Mr. Tony Sullivan
Mr. Howard West

Raymond/Bauer
365 Passaic Street
Rochelle Park, New Jersey 07662
Phone: 201/368-5700

Mr. Edward P. Forte
Mr. Paul Scheller

Franki Foundation Company
920 Statler Office Building
Boston, Massachusetts 02116
Phone: 617/426-4369

Mr. Richard Pizzi
Dr. William Neely

Cementation Piling & Foundations, Ltd.
7335 North Oracle Road
Tucson, Arizona 85704
Phone: 602/293-2990

Mr. P. Cochran

EUROPE

Cementation Piling & Foundations, Ltd Cementation House Maple Cross, Rickmansworth Hertfordshire WD3 2SW ENGLAND	Mr. David Greenwood Mr. Graham Thomson
Landesgewerbeanstalt Bayern Gewerbemuseumsplatx 2 8500 Nurnberg 1 W. GERMANY	Dr. Klaus Hilmer
GKN Keller Ltd., U.K. Division GKN Keller Foundations Oxford Road, Ryton-on-Dunsmore Coventry CV8 3EG ENGLAND	Dr. J. Michael West Mr. Klaus Kirsch Mr. Volker Baumann Dr. Gerhardt Chambosse (Munich) Mr. Heinz Priebe
Thorburn and Partners 145 West Regent Street Glasgow G2 45A SCOTLAND	Mr. Sam Thorburn Mr. Tom Hindle
Institute for Grundbau Bodenmechanik Paul Gerhardt Allee 2 8 Munchen W. GERMANY	Dr. Koreck
Building Research Establishment Garston, Watford WD2 7JR ENGLAND	Dr. Andrew Charles
Karl Bauer Spezialtiefbau GmbH Wittelsbacherstrasse 5 8898 Schrobenhausen W. GERMANY	Mr. Guenther Oelckers Fritz Pollens, KG Halberstadterstr. 6, 1000 Berlin 31, W. Germany
Vibroflotation (UK) Ltd. P. O. Box 94 Beaconsfield Buckinghamshire HP9 1BU ENGLAND	Mr. Peter Thomson
Franki 196, Rue Gentry B4020 Liege Belgigue	Mr. Maurice Wallays

ASIA

(Sand Compaction Piles)

Dr. Hisao Aboshi
Professor
University of Hiroshima
3-8-2, Sendamachi, Nakaku
Hiroshima, JAPAN

Kensetsu Kikai Chosa Co., Ltd,
8th Floor, Takahashi Minami Bldg.
3-14-16, Nishitenma, Kita-Ku,
Osaka, JAPAN
Mr. Y. Mizutani

Fudo Construction Co.
4-25, Naka-Ku, Sakee-Cho
Hiroshima, JAPAN
Mr. Toyohiko Abe

Nippon Kokan KK
Tsurumi Works
No. 1, 2-Chome, Suehiro-Cho
Tsurumi-Ku, Yokohama,
JAPAN T230
Mr. Miura Yuhichi
Mr. Masatoshi Shimizu

Dubon Project Engineering Pvt., LTD.
2, Rehem Mansion, 1st Fl., 44,
S. Bhagat Singh Rd.
Bombay, INDIA 40039
Mr. K. R. Datye
Mr. Bhide
Mr. S. S. Nagaraju

APPENDIX B: LOCAL BEARING FAILURE OF AN ISOLATED STONE COLUMN

1. Stone columns are an effective method for resisting rotational shear failures involving soft clays in embankments and slopes (DiMaggio 1978†). For a conventional slope stability analysis, the resisting shear force F developed by the stone column is determined by multiplying the effective normal force, $\bar{W}_N$, acting on the shear surface by the tangent of the angle of internal friction of the stone, $\tan \phi_s$. The shear capacity, F, of the stone column can, under unfavorable conditions, be limited by a local bearing failure†† of the stone column and cohesive soil behind the column as illustrated in Figures B1 and B2.

2. Now consider the behavior of an isolated, single stone column surrounded by a cohesive soil. If the shear force in the stone column is sufficiently large compared to the strength of the surrounding cohesive soil, a secondary failure surface can develop in the stone column extending downward from the circular arc failure surface (Figure B1). The resulting wedge of failed stone is bounded above by the circular arc failure surface. The lower failure surface develops within the stone at an angle resulting in the minimum resistance to sliding as defined by force F. The shear force F applied to the top causes the wedge (Figure B2) to slide downward and laterally in the direction of movement of the unstable soil mass above. Sliding of the wedge of stone is resisted by the frictional resistance of the stone developed along the bottom of the wedge and the passive lateral resistance of the adjacent clay. If the passive resistance of the clay is not sufficient, the stone wedge undergoes a local bearing failure by punching into the clay. If a local bearing failure of the clay occurs behind the stone column, the capacity of the column is limited by the secondary wedge failure. A local bearing failure of the clay behind the stone column has been observed by Goughnour (1981) during a direct shear test performed in the field on a stone column. Reduced strength of the composite mass was also indicated at Santa Barbara (Engelhardt and Golding 1975) and Steel Bayou (Ehrgott 1977).

Note: Equation, table, or figure numbers with an asterisk refer to the Federal Highway Administration Stone column report (Barksdale and Bachus 1983).

† References cited in this Appendix can be found on the last page.

†† Personal communication, September 1981, between R. R. Goughnour and R. D. Barksdale.

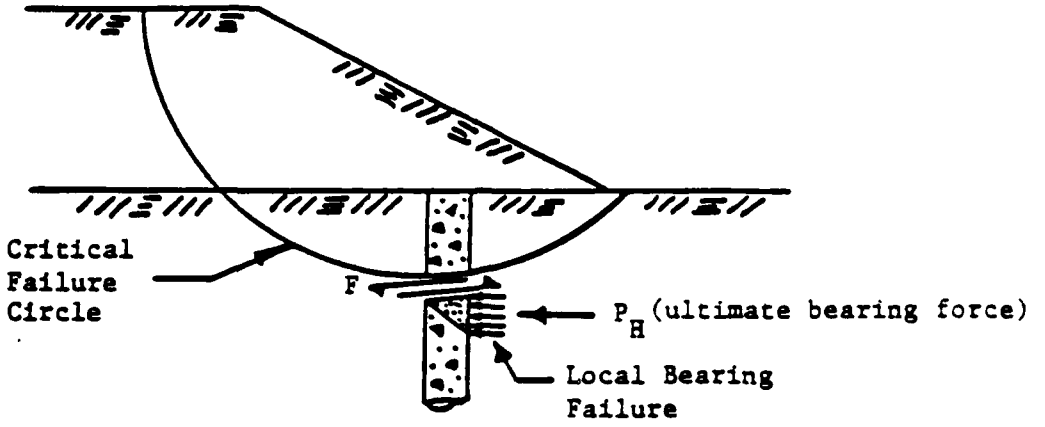

Figure B1. Wedge type local bearing failure of a stone column

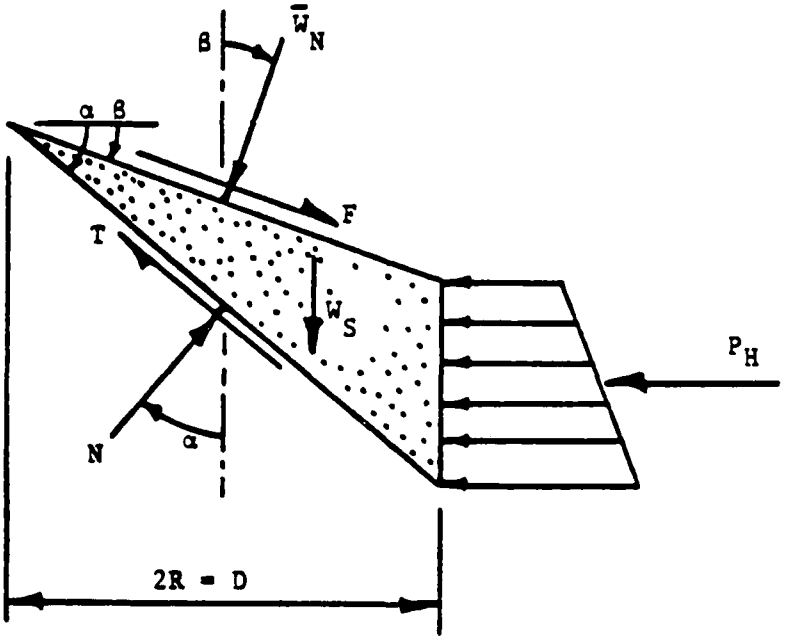

Figure B2. Local bearing capacity failure wedge in stone column

Local Bearing Failure

3. The limiting shear force that can be applied if a bearing failure controls can be obtained for an isolated column by considering the equilibrium of the wedge shown in Figure B1. This wedge together with the forces acting on it are illustrated in Figure B2. The following symbols used in these figures, as well as in subsequent derivations, are listed in the Notation (Appendix G):

W_s = effective force of stone in the wedge

$\bar{\gamma}_s$ = effective (bouyant) unit weight of stone in wedge

P_H = ultimate lateral resistance of the clay acting on the wedge

N,T = normal and shear force, respectively, exerted on the bottom surface of the wedge

$\bar{W}_N$,F = normal and shear force, respectively, exerted on the top surface of the wedge

R = radius of the stone column

D = diameter of the stone column

ϕ_s = angle of internal friction of the stone column

α,β = angle of inclination of the lower and upper surfaces of the wedge, respectively

4. The upper surface of the wedge makes an angle β with the horizontal†. This upper surface coincides with the circular arc failure surface (Figure B1). The lower surface of the wedge makes an angle of α with the horizontal. Now consider equilibrium of the wedge. To develop the required relationship for F , first sum forces acting on the wedge in the vertical direction and solve for the unknown normal force N acting on the bottom of the wedge obtaining.

$$N = \frac{W_s + \bar{W}_N \cos \beta + F \sin \beta}{\cos \alpha + \tan \phi_s \sin \alpha} \qquad \text{(B1)}$$

where the forces and angles are shown in Figure B2.

---

† R. R. Goughnour of the Vibroflotation Foundation Company has previously developed a solution similar in concept for the special case of $\beta = 0$. His solution handled lateral pressure on the column slightly differently than this solution.

5. Now sum the forces acting on the wedge in the horizontal direction, substitute for the unknown force N using Equation B1, and solve for the limiting force F obtaining

$$F = \frac{W_N (\sin \beta + \lambda \cos \beta) + \lambda W_s + P_H}{\cos \beta - \lambda \sin \beta} \tag{B2}$$

where

$$\lambda = \frac{\tan \phi_s \cos \alpha - \sin \alpha}{\cos \alpha + \tan \phi_s \sin \alpha}$$

$$W_s = \pi (\tan \alpha - \tan \beta) R^{3-} \gamma_s$$

6. In the derivation of Equation B2, the effects of adjacent stone columns and outward, lateral spreading of the stone columns were neglected. Neglecting the effect of adjacent columns should introduce a factor of conservation in predicting the effect of a local bearing failure (Broms 1964). These effects are offset by neglecting lateral spreading which should be on the unconservative side.

Lateral Bearing Failure in Cohesive Soil

7. The ultimate passive pressure developed by the cohesive soil as the wedge pushes against it can be calculated using the theory presented by Broms (1964) for a single, laterally loaded pile embedded in a frictionless soil. As shown in Figure B3, the ultimate lateral pressure q_h at the surface is taken to be $q_h = 2c$ with the resistance increasing linearly over a depth of three pile diameters where it reaches a maximum limiting value of $q_h = 9c$. The total depth beneath the surface $h + z_o$ (Figure B4) is considered in determining the three pile diameters. Near the surface, the failure occurs because of the upward flow of cohesive soil toward the surface. With increasing depth the failure becomes one of the plastic flow of the soil from the front of the pile around the sides (Figure B3).

8. For a single rough pile, plastic theory (Poulos and Davis 1980; Meyerhof and Chaplin 1953) indicates that below a depth of approximately three diameters the ultimate lateral capacity is about $q_h = 11$ to $12c$. Use of

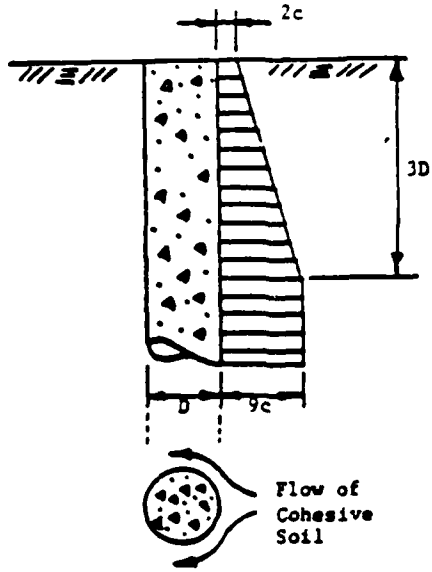

Figure B3. Bearing capacity of a rigid pile translating laterally in a cohesive soil

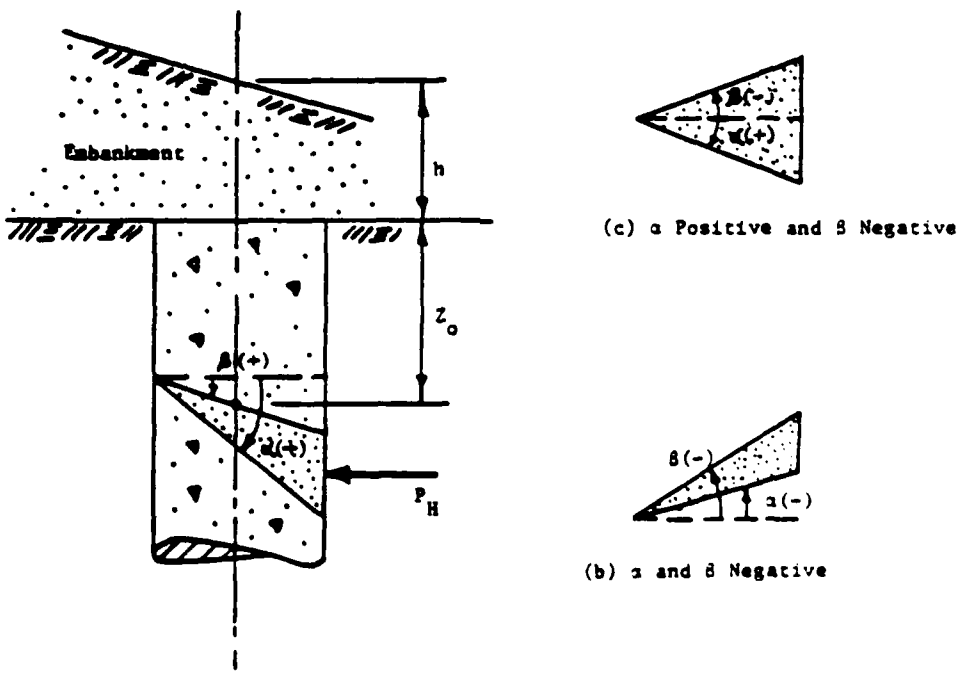

Figure B4. Notation used in formulas for local bearing failure of a stone column

an ultimate resistance of 9c, however, is felt to be prudent although it may be slightly on the conservative side. Further, the use of $q_h = 9c$ is reasonable since it is equal to the end bearing capacity of deep piles embedded in a cohesive soil. The value of $q_h = 2c$ used at the surface is also realistic since it equals about 40 percent of the bearing capacity of the clay in the vertical direction.

9. Now consider the ultimate lateral pressure developed on a wedge of stone making an angle α and β with the horizontal as shown in Figure B2. Using the pressure distribution shown in Figure B3, the ultimate passive pressure developed in the clay for a depth $(h + z_o) \leq 3D$ as illustrated in Figure B4 is

$$P_H = \frac{14}{3} Rc\Psi[h + z_o + R(1.714 + \tan \alpha)] \quad (B3)$$

and for a depth $h + z_o > 3D$

$$P_H = 36R^2 c\Psi \quad (B4)$$

where

R = radius of stone column

c = cohesion of soil

$\Psi = \tan \alpha - \tan \beta$

h = depth of fill above the stone column

z_o = depth of the circular arc failure surface below the top of the stone column

The sign convention used for α and β is shown in Figure B4. Once a trial circular arc failure surface has been selected, the value of β is known. The angle α is then determined to give the minimum value of shear force F that can be applied to the top of the wedge before a bearing failure occurs.

Calculation of Limiting Shear Force

10. The limiting shear force F in each column for a given circular arc sliding surface is calculated as follows:

a. Determine the angle β for a critical circle and calculate the effective normal force, $\bar{W}_N$ (Figure B4) at the point on the stone column where the circular arc intersects the center of the stone column (Figure B1).

b. Select at least three trial values of the angle of inclination α of the lower surface of the wedge.

c. For each value of α calculate the ultimate lateral soil resistance, P_H, using Equation B3 or B4 and a representative value of the undrained shear strength c of the cohesive soil.

d. For each value of α, calculate F for a bearing failure in the cohesive soil using Equation B2.

e. Plot the shear force F obtained from Equation B2 as a function of α and select the minimum value of F.

f. Calculate the shear force F that can act on the column if a local bearing failure does not develop: $F = \bar{W}_N \tan \phi_s$.

g. If a local bearing failure of the clay controls, the force calculated in Step e will be less than that calculated in Step f. In the stability analysis, use the smaller of these forces (or reduce the value of ϕ_s used in design).

h. Repeat the analysis for several selected points along the failure surface.

Design Charts

11. Figures B5 through B15 present graphically the solution for local bearing failure of a single, isolated stone column for selected design parameters. The procedure for using the charts is as follows:

a. Select tentative design parameters and perform a stability analysis for the stone column improved ground. Plot the critical circle through the stone columns. Examine for the possibility of local failure several points along the critical circle where it intersects the center of the columns. Measure the inclination β of the circle (with the correct sign) and the depth $h + z_o$ of each point (Figure B4).

b. Calculate the effective vertical force $\bar{W}_v$ acting on the stone column at the depth under consideration by multiplying the vertical effective stress times the area of the stone column. First, calculate the effective body stress due to the stone column at the selected point. Use the bouyant unit weight of the stone below the groundwater table. Then calculate the vertical stress σ due to the embankment above the stone column and obtain the stress concentration in the column using $\sigma_s = \mu_s \sigma$ Equation 8b*. Add the body stress to σ_s and multiply by the area of the stone column to obtain $\bar{W}_v$.

c. Using $\bar{W}_v$ from Step b and the design value(s) of ϕ_s and the cohesion of the clay c, enter the appropriate figure and estimate the value of the reduction factor n.

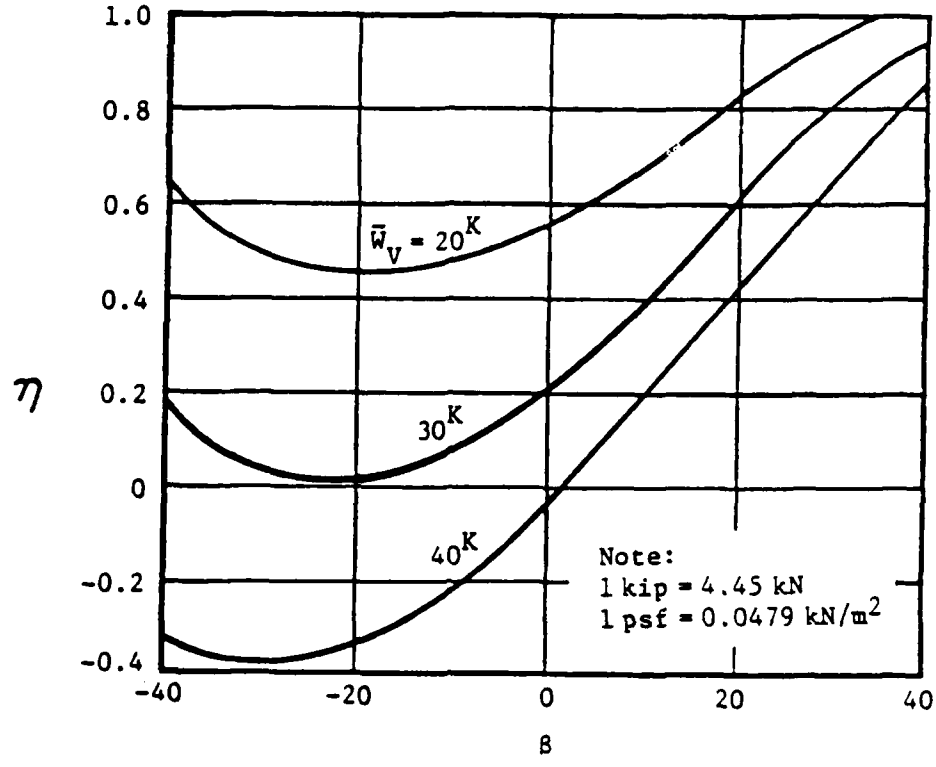

Figure B5. Local bearing failure stability reduction factors for deep failure: $\phi_s = 30°$, c = 100 psf

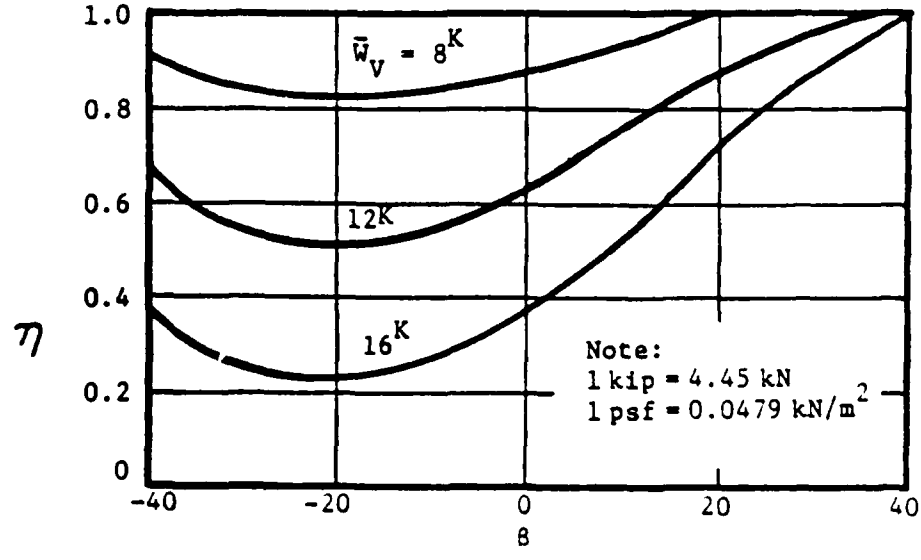

Figure B6. Local bearing failure stability reduction factors for shallow failure: $\phi_s = 30°$, c = 100 psf

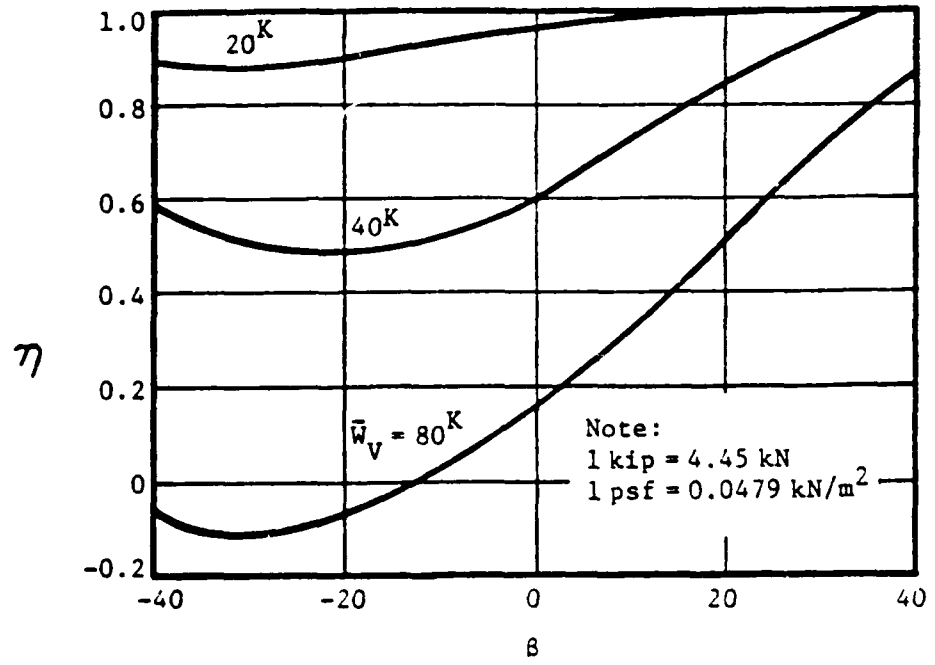

Figure B7. Local bearing failure stability reduction factors for deep failure: $\phi_s = 36°$, c = 200 psf

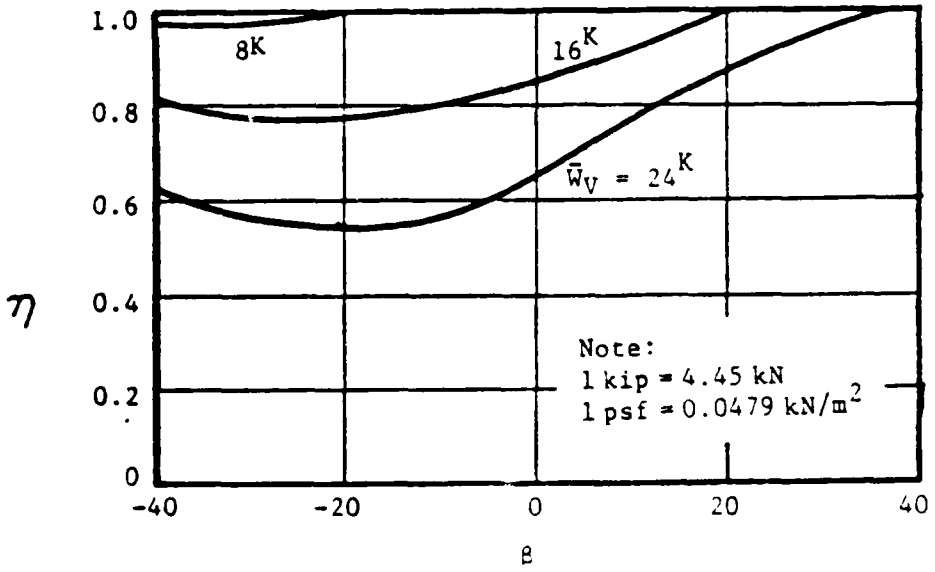

Figure B8. Local bearing failure stability reduction factors for shallow failure: $\phi_s = 36°$, c = 200 psf

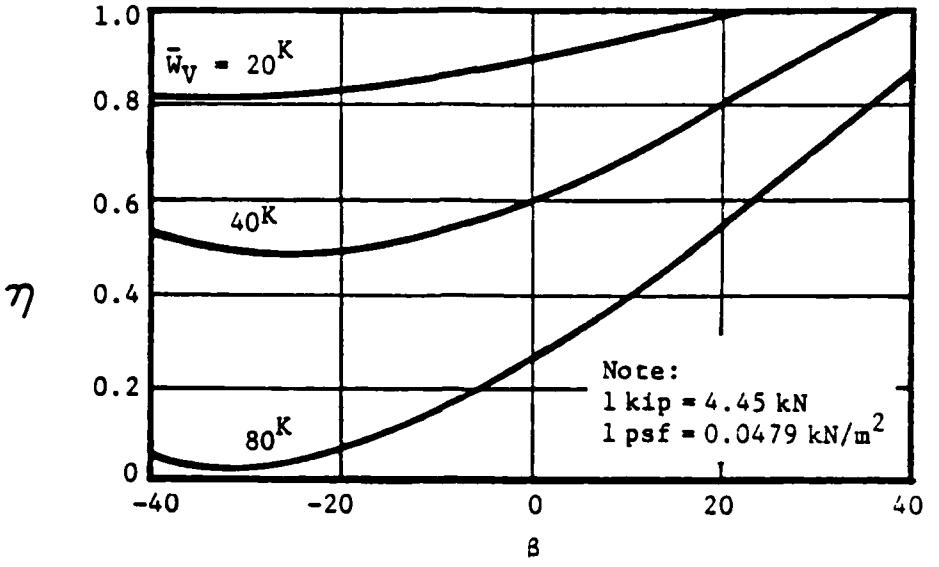

Figure B9. Local bearing failure stability reduction factors for deep failure: ϕ_s = 42° , c = 200 psf

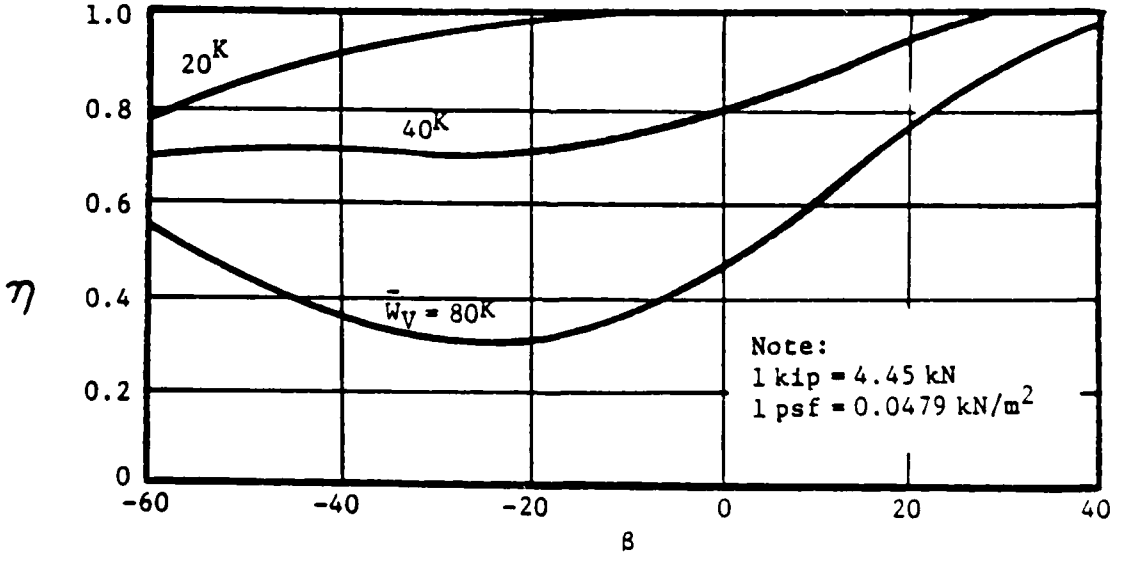

Figure B10. Local bearing failure stability reduction factors for deep failure: ϕ_s = 42° , c = 300 psf

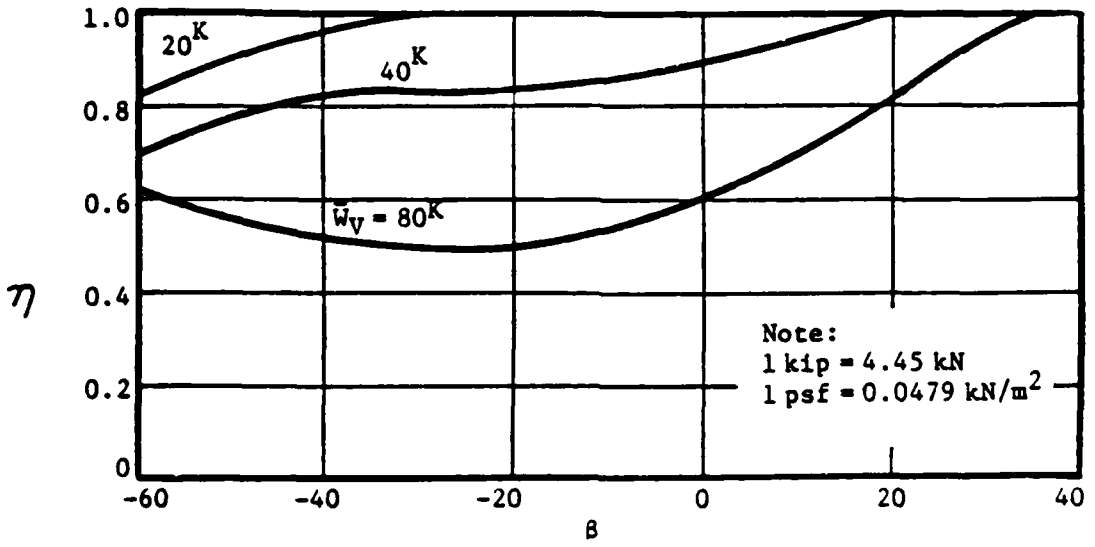

Figure B11. Local bearing failure stability reduction factors for deep failure: $\phi_s = 42°$, c = 400 psf

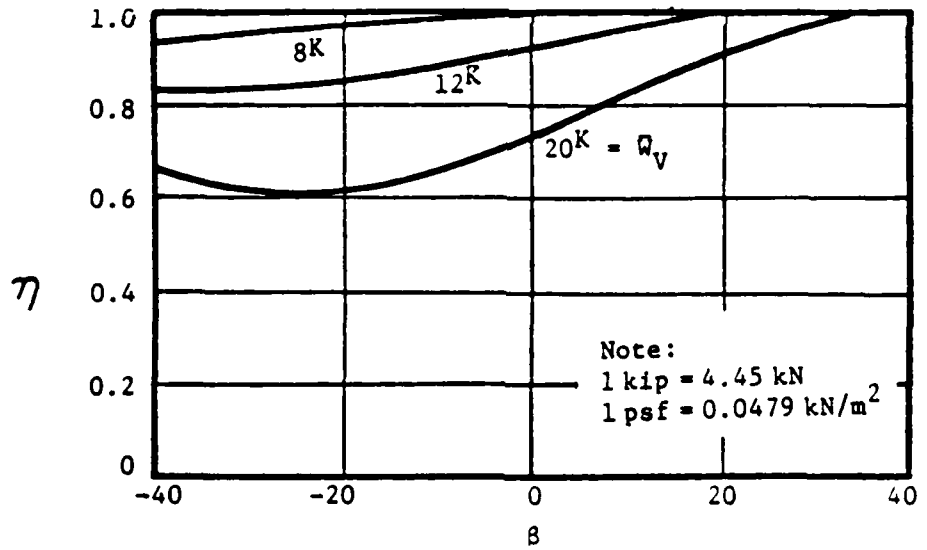

Figure B12. Local bearing failure stability reduction factors for shallow failure: $\phi_s = 42°$, c = 200 psf

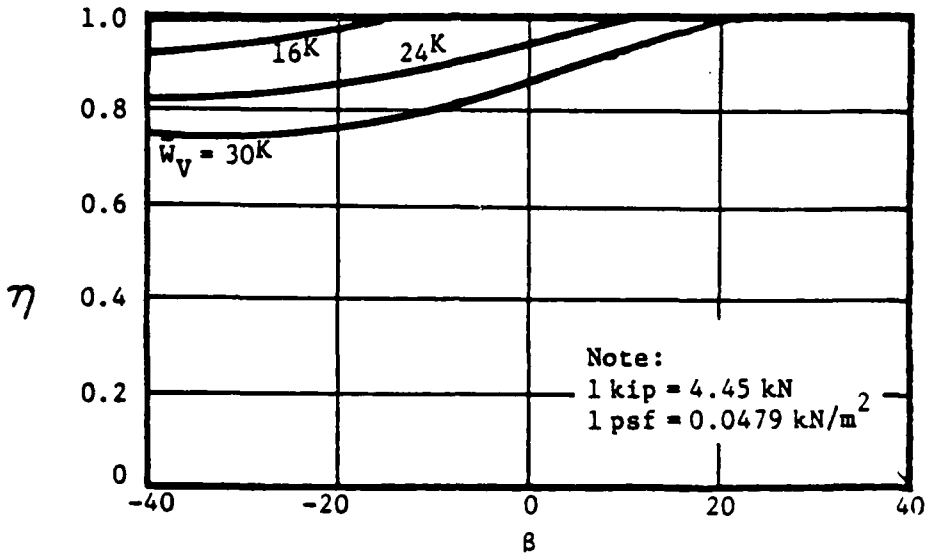

Figure B13. Local bearing failure stability reduction factors for shallow failure: $\phi_s = 42°$, c = 400 psf

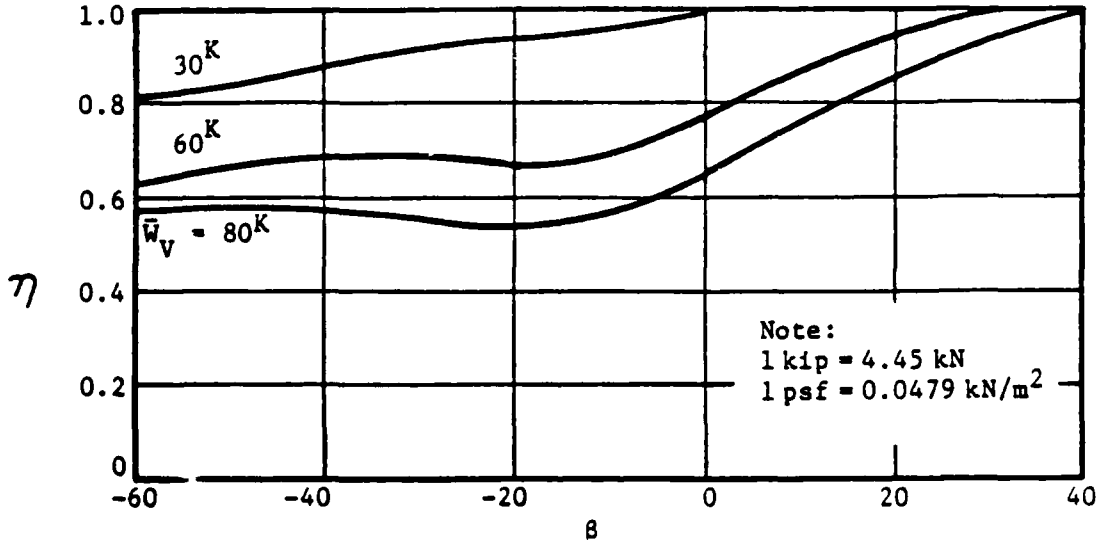

Figure B14. Local bearing failure stability reduction factors for deep failure: $\phi_s = 45°$, c = 600 psf

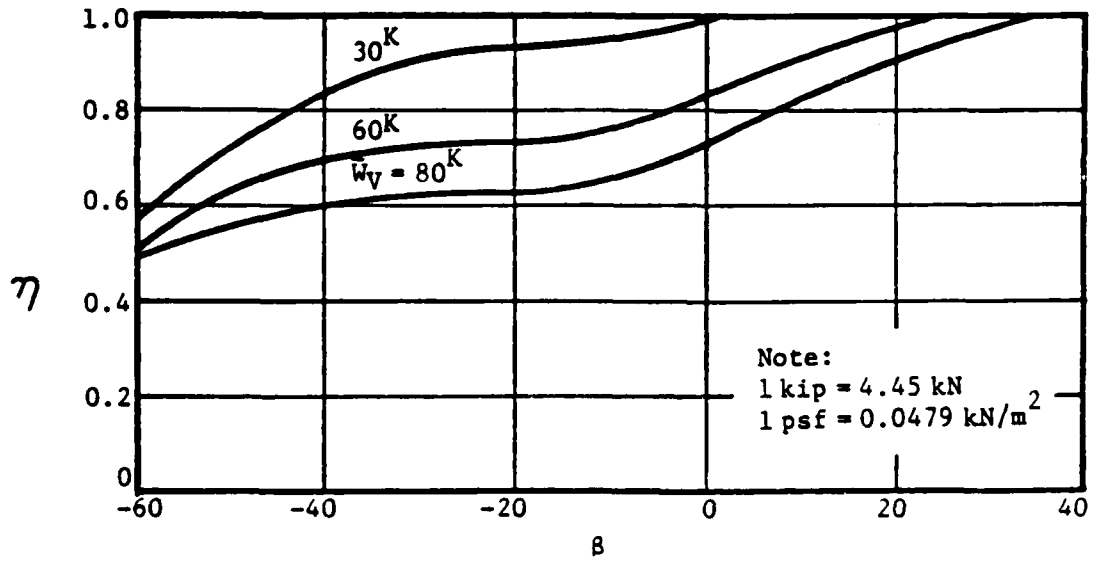

Figure B15. Local bearing failure stability reduction factors for deep failure: $\phi_s = 50°$, c = 800 psf

d. The "deep" charts should be used when the combined embankment height and stone column depth $h + z_o$ is equal to or greater than three stone column diameters; otherwise the "shallow" charts should be used.

12. The ratio η, obtained from these figures, is defined as follows:

$$\eta = \frac{F \text{ (from Equation B2)}}{\bar{W}_N \tan \phi_s} \tag{B5}$$

Physically η is the ratio of resisting force that is developed by an isolated stone column if a local bearing failure occurs to the force developed if local failure does not occur (i.e., the force that conventionally would be used in a stability analysis). Hence, η is the reduction factor indicating when a local bearing failure may become a problem for the given geometry and material properties used in the design. Theoretically, when $\eta < 1$, local bearing controls the maximum resisting force and moment that can be developed by the stone column. A reduction in resisting force (and moment) developed by the stone column would result in a reduction if safety factor of the slope compared to that computed for a general shear failure.

Design

13. Full-scale and model direct shear tests indicate a local bearing

failure of at least a single stone column is possible. The analysis including the design curves just presented is for a single, isolated stone column. The relatively close proximity of adjacent stone columns and lateral spreading greatly complicate the actual problem compared with an isolated column; certainly further field and model tests are needed in addition to more refined theories. Nevertheless, the design charts and theory presented can be used to indicate when local bearing failure may be a problem. Further, the proposed approach is useful as a general guide in design for selecting safe design parameters (ϕ_s, n).

14. The likelihood of a local bearing failure increases as the shear strength of the clay decreases, and as a greater angle of internal friction ϕ_s and stress concentration factor n are used in design. For example, if a ϕ_s of 42° is used, a local bearing <u>might</u> occur in cohesive soils having undrained shear strengths less than about 400 psf. (Examine Figures B9 through B13 for typical values of β and $\bar{W}_v$.) A local bearing failure could occur in higher strength cohesive soils if ϕ_s values greater than 42° are used in design. Therefore, when stability is being analyzed in very soft and soft cohesive soils, the effect of a local bearing failure on the overall slope stability should be considered. Also, in firm and stiff soils such an analysis may show that use of higher values of ϕ_s may be possible without undergoing a local bearing failure.

15. Local bearing failure can be easily handled in a slope stability analysis using the concept of a limiting angle of internal friction ϕ_s of the stone. Using this simplified approach, several representative points are selected along the critical failure circle(s) as determined by a stability analysis on the stone column improved ground. The effective vertical stress $\bar{W}_v$ and inclination of the failure circle β (with correct sign) at the selected points are determined. Figures B8 through B15 can then be used to determine if a local bearing failure might occur at the selected points (and the actual magnitude of the reduction in the resisting shear force F). If a local failure is found not to occur over a significant portion of the failure surface, the design is satisfactory; otherwise consideration should be given to reducing ϕ_s. Note that the figures indicate local failure in general may be a problem only when $\beta<0$ (i.e., near and to the outside of the toe of the slope). Also, and perhaps more importantly, the charts serve to indicate when local failure is not of concern. In any case, past experience and good

engineering judgment should be taken into consideration in estimating the stability of the slope.

REFERENCES

Barksdale, R. D., and Buchus, R. C. 1983. "Design and Construction of Stone Columns," Vol I, Federal Highway Administration, Report FHWA/RD-83/026.

Broms, B. B. 1964. "Lateral Resistance of Piles in Cohesive Soils," Soil Mechanics and Foundation Engineering Journal, American Society for Civil Engineers, Vol 90, No. SM2, pp 21-62.

DiMaggio, J. A., 1978. "Stone Columns - A Foundation Treatment (In Situ Stabilization of Cohesive Soils)," Demonstration Project No. 4-6, Federal Highway Administration, Region 15, Demonstration Projects Division, Arlington, Va.

Ehrgott, J. Q. 1977. "Field Shear Test on Stone Columns," Memorandum for Record (with enclosures), US Army Engineer Waterways Experiment Station, Vicksburg, Miss.

Engelhardt, K., and Golding, H. C. 1975. "Field Testing to Evaluate Stone Column Performance in a Seismic Area," Geotechnique, Vol 25, No. 1, pp 61-69.

Meyerhof, G. G., and Chaplin, M. A. 1953. "The Compression and Bearing Capacity of Cohesive Soils," British Journal of Applied Physics, Vol 4, pp 20-26.

Poulos, H. G., and Davis, E. H. 1980. Pile Foundation Analysis and Design, 1st ed., John Wiley, New York, pp 145-148.

APPENDIX C: EXAMPLE BEARING CAPACITY PROBLEMS

Bearing Capacity Example 1

1. Example 1 illustrates prediction of the load due to a wide fill that can be supported by stone column improved ground to avoid a shear failure of the stone columns. The specific problem is to determine what height of fill the stone column improved ground can safely support. Both a general shear failure and a local bulging failure in a deep, very soft clay layer (Figure C1) must be considered. The subsurface conditions and pertinent parameters needed to solve the problems are shown in Figure C1. Assume the stone column has an angle of internal friction ϕ_s of 42 deg, and an equilateral triangular pattern of columns is used having a spacing $s = 7$ ft .

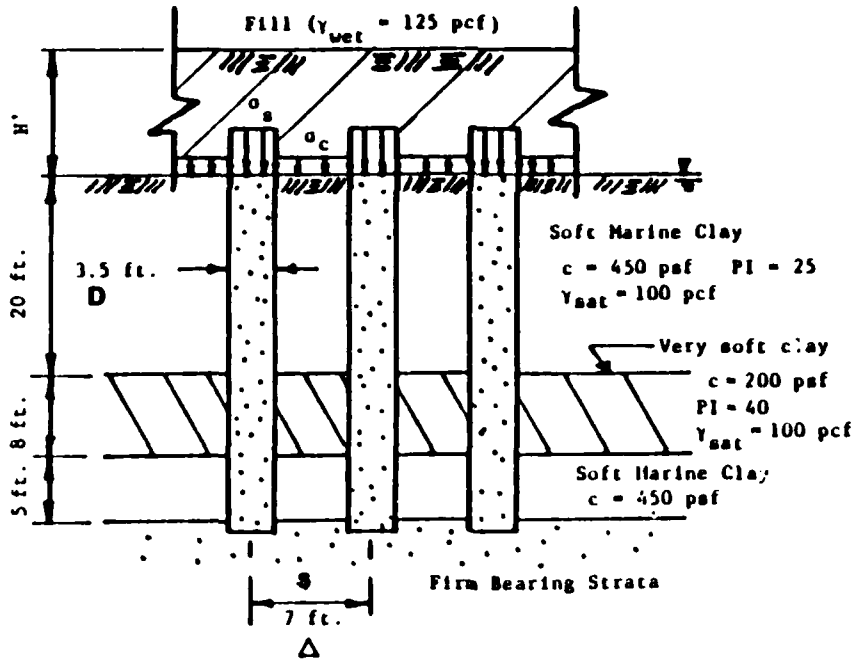

Figure C1. Bearing capacity Example 1--Wide Fill Over Stone Column Improved Clay

a. Area replacement ratio a_s . Calculate ratio a_s from Equation 5b*:

Note: Equation, table, or figure numbers with an asterisk refer to the FHWA Stone Column report (Barksdale and Bachus 1983).

$$a_s = 0.907\left(\frac{D}{s}\right)^2 = 0.907\left(\frac{3.5\ ft}{7\ ft}\right)^2 = 0.227 \qquad (5b)^*$$

$$A_s = \frac{\pi \cdot D^2}{4} = \frac{3.14\ (3.5\ ft)^2}{4} = 9.62\ ft^2 \qquad (C1)$$

$$A = \frac{A_s}{a_s} = \frac{9.62\ ft^2}{0.227} = 42.4\ ft\ (total\ area) \qquad (3)^*$$

where

A_s = stone column area

A = total area within the unit cell

b. Stone column. Estimate the general ultimate capacity of the stone column using Equation C2 assuming a bulging failure occurs in the upper three stone column diameters of depth. Since the clay has a PI < 30 and is not classified as very soft ($c < 250$ psf), use $\tilde{N}_c = 22$ (Chapter VII, Barksdale and Bachus 1983†).

$$\tilde{q}_{ult} = c\tilde{N}_c = 0.45\ ksf\ (22) = 9.9\ ksf \qquad (50)^*$$

$$P_{ult} = \tilde{q}_{ult}A_s = 9.9\ ksf\ (9.62\ ft^2) = 95.2\ kips \qquad (C2)$$

where

$\tilde{q}_{ult}$ = ultimate bearing capacity of stone column

c = cohesion of soil

$\tilde{N}_c$ = ultimate bearing capacity factor of stone column

In the above expressions, the stress in the stone column at ultimate is $\sigma_s = \tilde{q}_{ult} = c\tilde{N}_c$.

c. Deep bulging. Now check for the possibility of a bulging failure in the very soft clay stratum located at a depth of 20 ft. As discussed in Appendix B, the ultimate lateral stress which an isolated stone column can develop is approximately equal to $\sigma_3 \cong 9c = 9(0.2\ ksf) = 1.8\ ksf$ since the weak stratum is greater than 3D below the surface. From Equation 9* the ultimate stress the stone column can carry is then

$$\tilde{q}_{ult} = \sigma_3 \frac{(1 + \sin \phi_s)}{(1 - \sin \phi_s)} = 1.8\ ksf\ (5.04) \qquad (9)^*$$

$$\tilde{q}_{ult} = 9.07\ ksf$$

---

† References cited in this Appendix can be found on the last page.

where σ_3 equals minor principle stress. Since the ultimate stress the stone column can carry considering a deep bulging failure in the very soft layer is slightly less than for a failure at the surface, the very soft deep stratum controls.

d. Cohesive soil. The maximum ultimate stress that the clay surrounding the stone column can take is $\sigma_c = 5c = 5(0.450 \text{ ksf}) = 2.24$ ksf. However, the total load applied to the unit cell must also not overload the clay. Assuming a stress concentration factor $n = 3$, from Equations 8a* and 8b*

$$\mu_s = \frac{n}{[1 + (n - 1)\, a_s]} = \frac{3}{[1 + (3 - 1)\, 0.227]} = 2.06 \qquad (8b)^*$$

$$\mu_c = \frac{1}{[1 + (n - 1)\, a_s]} = \frac{1}{[1 + (3 - 1)\, 0.227]} = 0.688 \qquad (8a)^*$$

Then

$$\sigma_c \leq \mu_c \sigma = \mu_c \left(\frac{\sigma_s}{\mu_s}\right) \qquad (C3)$$

$$\sigma_c < \mu_c \sigma = 0.688 \left(\frac{9.07 \text{ ksf}}{2.06}\right) = 3.0 \text{ ksf}$$

where

σ_c = average stress acting over soil in unit cell

μ_c = ratio of stress in cohesive soil to average stress

σ_s = average stress acting over stone column

μ_s = ratio of stress in stone column to average stress

Since 3.0 ksf is greater than $5c = 2.25$ ksf, $\sigma_c = 5c = 2.25$ ksf is the ultimate stress the clay can carry.

e. Allowable fill loading. The ultimate loading that can be applied over the unit cell area well within the fill area is

$$P_{ult} = \sigma_s A_s + \sigma_c A_c = (9.07 \text{ ksf})(9.62 \text{ ft}^2) + (2.25 \text{ ksf})(32.8 \text{ ft}^2) \qquad (C4)$$

$$P_{ult} = 161 \text{ kips}$$

Using a safety factor of 2.0 the allowable loading is $P_{all} = 161 \text{ kips}/2 = 80.5$ kips. The height of embankment H', that will apply the safe loading to the unit cell is $\gamma_{wet}^{fill} H' = \sigma = P_{all}/A$.

Hence

$$H' = P_{all}/(\gamma_{wet}^{fill} A) = \frac{80.5 \text{ kips}}{(0.125 \text{ kcf} \times 42.4 \text{ ft}^2)} \quad \text{(C5)}$$

$H' = 15.1$ ft

f. Commentary. Settlement of the fill would be significant and should be calculated. Also, the stability at the edge of the fill should be checked using a circular arc analysis. In this example the very soft clay layer at a depth of 20 ft controls the load that can be applied to the stone columns. Use of an ultimate lateral stress of 9c acting on the stone columns should give a conservative, but realistic, estimate of the ultimate resistance to bulging that can be developed (refer to Appendix B for a more indepth consideration of this aspect).

Using $\sigma_3 = 9c$ as the limiting lateral pressure that the soil can withstand, the ultimate load that a stone column can carry would for $\phi_s = 42°$ be equal for depths greater than 3D to $\tilde{q}_{ult} = 9c\ (1 + \sin \phi_s)/(1 - \sin \phi_s) = 9c\ (5.04) = 45c$ or $\tilde{N}_c = 45$, which indicates that a limiting value of $\tilde{N}_c$ exists at a deep depth.

Since the fill is wide, the stress on the stone column does not decrease with depth because of lateral spreading of stress. If a narrow group of stone columns had been used, the stress would, however, decrease with depth; this could be taken into account to determine the increased stress that could be applied at the surface compared with the level of the very soft clay stratum which controlled.

Finally, Vesic (1972) cavity expansion theory could also have been used to determine the ultimate capacity of the stone column in the weak stratum. Since the clay is very soft and has a PI > 30, $E = 5c$ is used to calculate a Rigidity Index, I_r (Equation 13*) of 1.72 for $\nu_s = 0.45$. In this analysis let q equal the total lateral stress acting at the center of the soft layer. Nonlinear finite element analyses indicate the lateral pressure due to the applied surface loading σ_c can be conservatively approximated as $0.4\sigma_c$:

$$q = K_o \gamma z + 0.4\sigma_c = 0.75(24 \text{ ft})(0.1 \text{ kcf}) + 0.4\ (2.25 \text{ ksf}) \quad \text{(C6)}$$

$q = 2.7$ ksf

Now $F_c' = \ln I_r + 1 = \ln 1.72 + 1 = 1.54$ for $\phi_c = 0$, Figure C2 (16*), and no volume change. Then the ultimate load the stone column can carry is

$$q_{ult} = (cF_c' + qF_q') \frac{(1 + \sin \phi_s)}{(1 - \sin \phi_s)} \quad (14)*$$

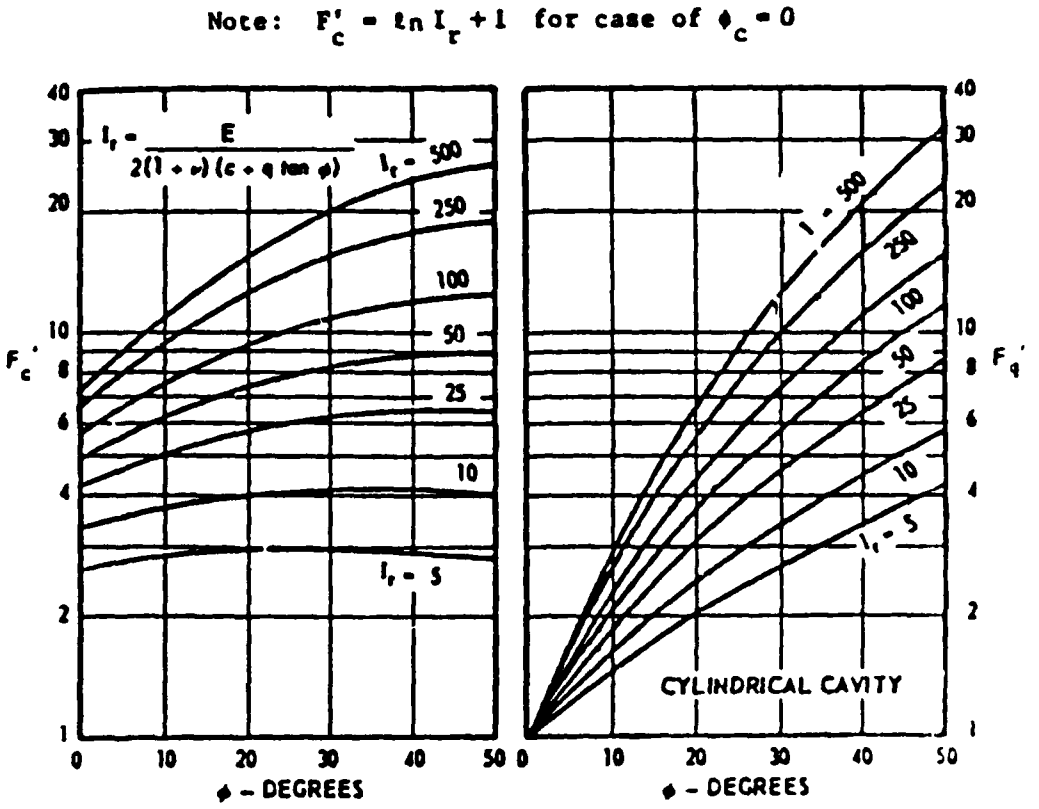

Figure C2. Vesic cylindrical cavity expansion factors (Vesic 1972)

$$\tilde{q}_{ult} = [0.2 \text{ ksf } (1.54) + 2.7 \text{ ksf } (1)][5.04] = 15.1 \text{ ksf}$$

where F_c' and F_q' are Vesic cavity expansion factors.

Because of the large effect of overburden pressure, cavity expansion theory appears to overestimate the load which the stone column can carry through the very soft clay stratum.

Bearing Capacity Example 2

2. Stone columns are to be used to improve a stiff clay to slightly reduce settlement of a foundation 13.5 by 10.5 ft in plan (Figure C3). The modular ratio between the stone columns and the surrounding clay is estimated to be 6.0. Determine the ultimate and safe bearing capacity of the 10 stone column group illustrated in Figure C3. The material properties and geometries involved are shown on the figure.

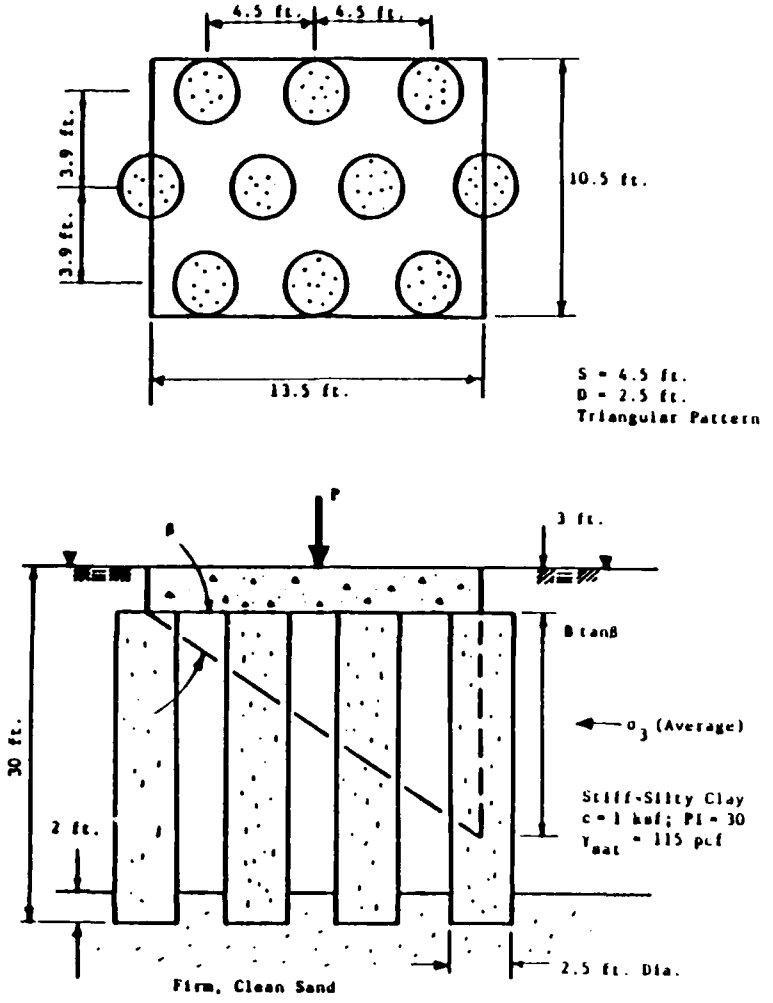

Figure C3. Bearing capacity Example 2--Square Group

3. From Figure C4 (27*) the stress concentration factor in the stone column improved ground is about 2.0. The bearing capacity calculations are as follows:

a. Calculate the area replacement ratio, a_s

$$A_s = \frac{3.14}{4} (2.5 \text{ ft})^2 \times 10 = 49.1 \text{ ft}^2 \quad \text{(C7)}$$

$$A = 13.5 \text{ ft} \times 10.5 \text{ ft} = 141.8 \text{ ft}^2 \quad \text{(C8)}$$

$$a_s = \frac{A_s}{A} = \frac{49.1 \text{ ft}^2}{141.8 \text{ ft}^2} = 0.346 \quad \text{(C9)}$$

b. Determine the stress concentration ratio in the stone column from Equation 8b* or Figure C5 (68*)

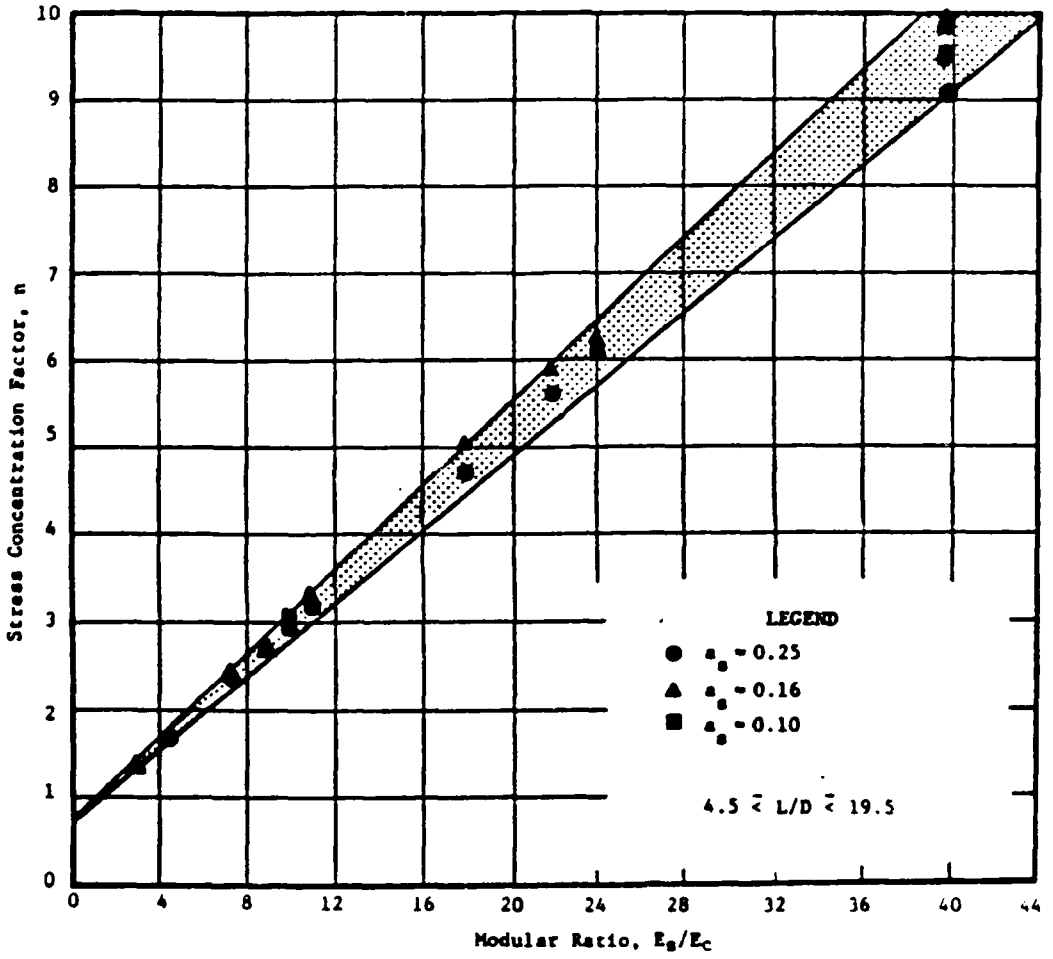

Figure C4. Variation of stress concentration factor with modular ratio--linear elastic analysis (Barksdale and Bachus 1983)

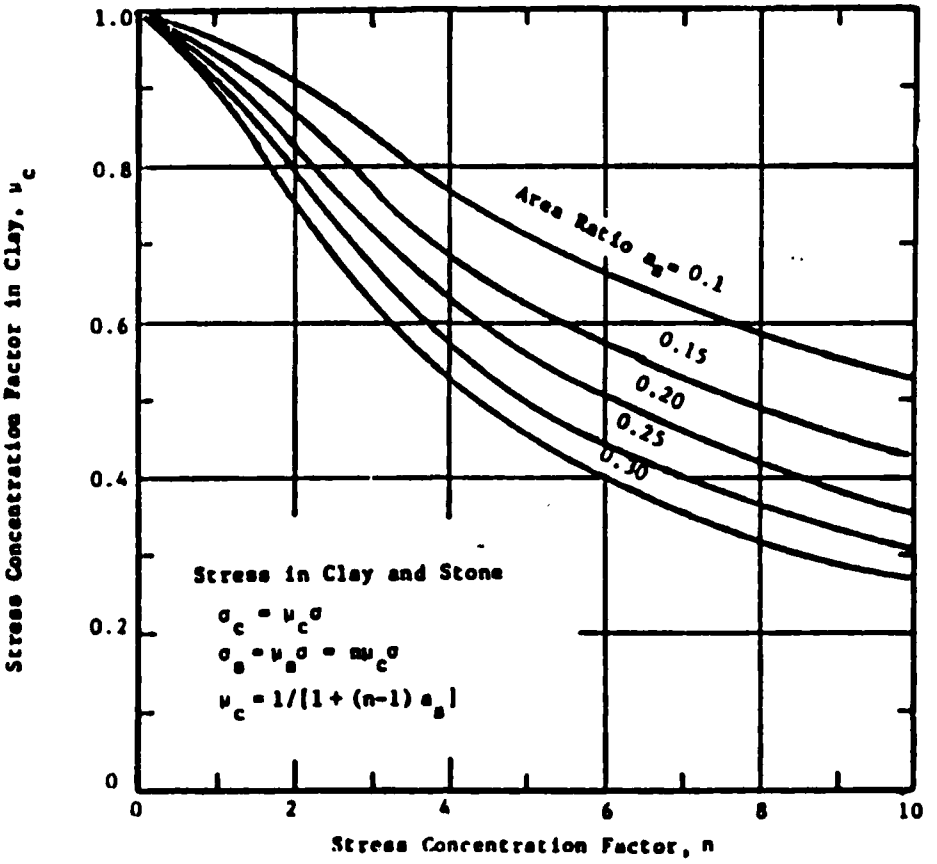

Figure C5. Variation of stress in clay with stress concentration factor and area ratio (Barksdale and Bachus 1983)

$$\mu_s = \frac{n}{[1 + (n - 1)\, a_s]} = \frac{2}{[1 + (2 - 1)(0.346)]} = 1.49 \qquad (8b)^*$$

c. Calculate the composite shear strength within the stone column group (Equations 16a* and 16b*) and related parameters as follows:

$$[\tan \phi]_{avg} = \mu_s \tan \phi_s \, (a_s) = (1.49)\ (\tan 42°) \times (0.346) = 0.464 \qquad (16a)^*$$

$$\phi_{avg} = \tan^{-1} (0.464) = 24.9° \quad \text{and} \quad \beta = 45 + \frac{\phi_{avg}}{2} \qquad (C10)$$

$$\tan \beta = 1.566 \quad \text{and} \quad \tan^2 \beta = 2.454 \qquad (C11)$$

$$c_{avg} = c \cdot (1 - a_s) = 1 \text{ ksf } (1 - 0.346) = 0.654 \text{ ksf} \qquad (16b)^*$$

d. Using Vesic cavity expansion theory, calculate the ultimate lateral stress σ_3 in the clay surrounding the stone column group. Since the clay is stiff, has no organics, and has a PI = 30, use E = 11c for calculating the Rigidity Index, I_r. The average diameter of the foundation is $B = \sqrt{4A/3.14} = 13.4$ ft. The depth of the failure wedge is then (Figure C3) B tan β + 3 ft = (13.4 ft)(1.566) + 3 ft = 24 ft. The initial lateral stress in the stiff silty clay surrounding the stone columns will be used as a conservative estimate of the mean stress q (Equation 12*), for use in the cavity expansion theory. The stiff silty clay is known to be normally consolidated. Therefore, from Lambe and Whitman (1969), $K_o \cong 0.6$ for the surrounding silty clay, and $q \cong 0.6$ (13.5 ft × 0.115 kcf) = 0.931 ksf. Now calculate the Rigidity Index (Equation 13*).

$$I_r = \frac{E}{2(1 + \nu)(c + q \tan \phi)} = \frac{11c}{2(1 + 0.45)(c + q \tan 0°)} \qquad (13)*$$

giving $I_r = 3.79$. From $F'_c = \ln I_r + 1$ for $\phi = 0$ and Figure C2 (16*), $F'_c = 2.33$ and $F'_q = 1.0$. Then calculate the ultimate lateral stress which can be developed by the surrounding silty clay:

$$\sigma_3 = cF'_c + qF'_q = 1 \text{ ksf } (2.33) + 0.931 \text{ ksf } (1.0) \qquad (12)*$$
$$= 3.26 \text{ ksf}$$

e. Calculate the ultimate vertical stress and load that can be applied over the rigid foundation (refer to Equation 19*):

$$q_{ult} = \sigma_1 = \sigma_3 \tan^2 \beta + 2c_{avg} \tan \beta = 3.26 \text{ ksf } (2.454)$$
$$+ 2(0.654 \text{ ksf})(1.566) \qquad (19)*$$

$$q_{ult} = 8.0 \text{ ksf} + 2.0 \text{ ksf} = 10.0 \text{ ksf}$$

The ultimate load that can be carried by the foundation is $P_{ult} = q_{ult} \times A = 10.0$ ksf (141.8 ft^2) = 1,418 kips. Using a safety factor of 2.0, the foundation can carry $P_{ult} = 1418$ kips/2.0 = 709 kips. This amounts to 70.9 kips (or 35.5 tons) per stone column if the silty clay is assumed not to carry any of the load. This level of loading is reasonable for a foundation where settlement is of concern, Table C1 (12*).

f. Settlement of course would control the design. A total load on the group of 709 kips would be used for a first settlement estimate. For this loading the average stress applied to the foundation is $\sigma = 709$ kips/141.8 ft^2 = 5 ksf. The probable

distribution of stress between the stone and soil for $n = 2$ would be

$$\sigma_c = \mu_c \sigma = 0.743 \text{ (5 ksf)} = 3.7 \text{ ksf} \quad \text{(C12)}$$

$$\sigma_s = \mu_s \sigma = 1.49 \text{ (5 ksf)} = 7.45 \text{ ksf} \quad \text{(C13)}$$

Since the ultimate stress of the stiff clay is about $6.2c = 6.2$ ksf, the stress level in the clay is not excessive. Using the proposed design, the ratio of the settlement of the treated to unimproved ground would be approximately $S_t/S \cong \mu_c = 0.74$ (refer to Equations 20*, 21*, and 22* and Figure C6 (19*)). Thus for the conditions analyzed, reduction in settlement on the order of 25 percent would be expected. For the given site conditions, use of a larger footing (without stone columns) should also be evaluated considering magnitude of settlements and the economics of the designs.

In general for the wet method, a stone column spacing less than 5 ft is not recommended; Example Problem 2 would therefore be an exception because of the presence of the stiff, silty clay.

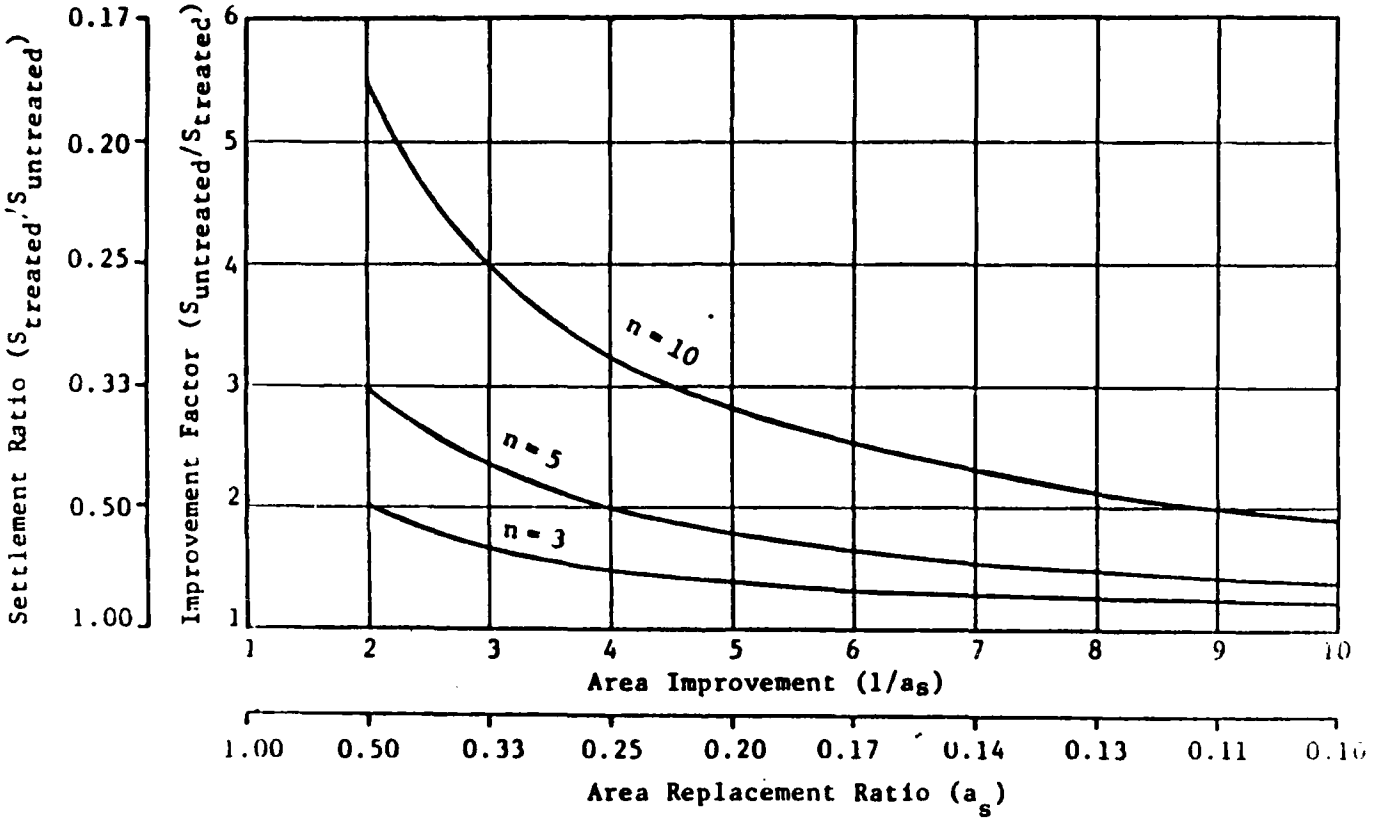

Figure C6. Maximum reduction in settlement that can be obtained using stone columns--equilibrium method of analysis (Barksdale and Bachus 1983)

Table C1

Approximate Range in Design Loads Used in Practice for Stone Columns (Barksdale and Bachus 1983)

Soil Type	Approximate Design Load, tons	
	Foundation Design[1]	Stability[1]
1. Cohesive soil[2]	15-30	20-45
400 psf ≤ c ≤ 600 psf		
600 psf ≤ c ≤ 1,000 psf	25-45	30-60
c > 1,000 psf	35-60	40-70
2. Cohesionless Soil	20-180 (see Note 1)	--

Notes:
1. In general, when stone column loads are given, all the applied load is considered carried by the stone column.
2. Typical design loads for foundations on cohesive soils are 15 to 30 tons.
3. Unit Conversions: 1 psf = 47.9 N/m^2 .

REFERENCES

Barksdale, R. D., and Bachus, R. C. 1983. "Design and Construction of Stone Columns," Vol I, Federal Highway Administration, Report FHWA/RD-83/026.

Lambe, T. W., and Whitman, R. V. 1969. Soil Mechanics, 1st ed., John Wiley, New York, pp 153-157.

Vesic, A. S. 1972. "Expansion of Cavities in Infinite Soil Mass," Journal of the Soil Mechanics and Foundation Engineering Division, American Society for Civil Engineers, Vol 93, No. SM3.

APPENDIX D: EXAMPLE SETTLEMENT PROBLEMS

Settlement Example 1

1. Settlement Example 1 illustrates calculating settlements of a soft clay reinforced with stone columns and loaded by a wide fill. The calculation of the load carrying capacity of stone column improved ground for a problem similar to this was illustrated by Example 1 in Appendix C. In the present example, primary consolidation settlements are calculated using both the equilibrium and finite element methods. Secondary settlements are also calculated. The problem is illustrated in Figure D1. The site consists of 20 ft of gray, soft silty clay overlying a firm to dense sand. The groundwater table is at the surface. An equilateral triangular pattern of stone columns

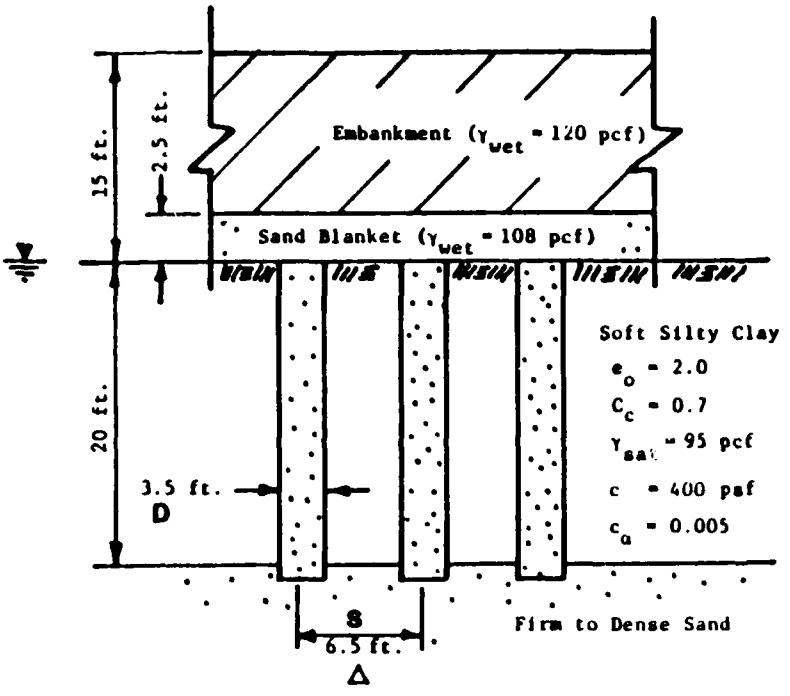

Figure D1. Settlement Example 1--Wide Fill Over Stone Column Improved Silty Clay

---

Note: Equation, table, or figure numbers with an asterisk refer to the Federal Highway Administration stone column report (Barksdale and Bachus 1983†).

† References cited in this Appendix can be found on the last page.

is used having a spacing of 6.5 ft. The diameter of the stone column is estimated from Table D1 (13*) to be 3.5 ft. A 2.5-ft sand blanket is to be placed over the soft silty clay for a working platform and drainage blanket.

Equilibrium method

2. The average stress σ exerted by the 2.5-ft sand blanket and 12.5-ft structural fill on the top of the stone columns is σ = 12.5 ft × 120 pcf + 2.5 ft × 108 pcf = 1,770 psf. The area replacement ratio a_s from Equation 5b* is for an equilateral, triangular stone column pattern:

$$a_s = 0.907 \left(\frac{D}{s}\right)^2 = 0.907 \left(\frac{3.5 \text{ ft}}{6.5 \text{ ft}}\right)^2 = 0.263 \qquad (5b)^*$$

Assume for the settlement analysis the stress concentration factor n to be 5.0. Then the stress concentration ratio μ_c in the clay is from Equation 8a* or Figure C5 (68*):

$$\mu_s = \frac{1}{[1 + (n - 1)\, a_s]} = 0.487 \qquad (8a)^*$$

The initial effective stress $\bar{\sigma}_o$ at the center of the silty clay layer is

$$\bar{\sigma}_o = 10 \text{ ft} \times (95 \text{ pcf} - 62.4 \text{ pcf}) = 326 \text{ psf} \qquad (D1)$$

The primary consolidation settlement in the clay layer from one-dimensional consolidation theory is from Equation 20*:

$$S_t = \frac{C_c}{1 + e_o} \log_{10}\left(\frac{\bar{\sigma}_o + \sigma_c}{\bar{\sigma}_o}\right) H \qquad (20)^*$$

$$S_t = \left(\frac{0.7}{1 + 2.0}\right) \log_{10}\left[\frac{326 \text{ psf} + (1770 \text{ psf})(0.487)}{326 \text{ psf}}\right] (20 \text{ ft} \times 12 \text{ in./ft})$$

$$S_t = 31.4 \text{ in.}$$

where

S_t = primary consolidation settlement occurring over a distance H of stone column treated ground

Table D1

Approximate Relationship Between Undrained Shear Strength and Completed Stone Column Diameter[1] (Barksdale and Bachus 1983)

Undrained Shear Strength, psf	Typical Diameter ft	Variation in Diameter			
		Approximate Completed Stone Column Diameter ft	Probe Diameter in.	Jetting Pressure psi	Comments
200	4.0 - 4.25	3.5	16 - 18	75 - 80	1 or 2 flushes
		3.5 - 4.0	18 - 19	75 - 80	1 or 2 flushes
		3.75 - 4.25	18 - 19	125 - 130	1 or 2 flushes
200 - 400	3.50 - 4.0	3.25	18 - 19	75 - 80	1 or 2 flushes
		3.5 - 3.75	18 - 19	125 - 130	1 or 2 flushes
		4.0	18 - 19	125 - 130	3 or 4 flushes
400 - 600	3.25 - 3.75	3.0	18 - 19	75 - 80	1 or 2 flushes
		3.25 - 3.5	18 - 19	125 - 130	1 or 2 flushes
		3.5 - 3.75	18 - 19	125 - 130	3 or 4 flushes
600 - 800[2]	3.0 - 3.25	2.5 - 3.0	16 - 18	75 - 80	1 or 2 flushes
		2.75 - 3.0	18 - 19	125 - 130	1 or 2 flushes
		3.0 - 3.25	18 - 19	125 - 130	3 or 4 flushes
800 - 1,000[2]	2.25 - 3.0	2.25 - 3.0	18 - 20	125 - 130	1 or 2 flushes

Notes:
1. The hole diameter formed by jetting is less than the diameter of the completed stone column.
2. In firm to stiff soils the hole is sometimes augered at greatly increased expense to achieve the required diameter. Augering is sometimes done for slope stability applications.
3. Unit Conversions: 1 psf = 47.9 N/m^2; 1 ft = 0.305 m; 1 psi = 6.89 kN/m^2.

C_c = compression index from one-dimensional consolidation test

e_o = initial void ratio

$\bar{\sigma}_o$ = average initial effective stress in the clay layer

σ_c = change in stress in the clay layer due to the externally applied loading, Equation 8a*

H = vertical height of stone column treated ground over which settlements are being calculated

The estimated primary consolidation settlement of the stone column improved silty clay layer is thus 31 in. following the equilibrium method. For comparison, the settlement in the silty clay layer if not improved with stone columns would be S = 45.2 in.

3. Note how simple the equilibrium method is to apply to a problem. The "trick," of course, is to estimate the correct value of stress concentration factor n to use in the analysis. In this problem, the fill was wide and no dissipation laterally of stress with depth occurs. The next settlement example shows how both the equilibrium and the finite element methods can be applied to a problem where the applied stress decreases with depth.

Nonlinear finite element method

4. Since the clay is soft and quite compressible use the nonlinear finite element method of analysis. First, calculate the modulus of elasticity E_c of the clay for the approximate stress range of interest. The initial average stress in the clay from the equilibrium method is $\bar{\sigma}_o$ = 326 psf. The change in stress in the clay due to the embankment loading is $\sigma_c = \mu_c \sigma$ = 0.487 (1,770 psf) = 862 psf. Using Table D2 (9*) and experience as a guide, the drained Poisson's ratio of the clay is assumed to be 0.42. From Equation 47* the modulus of elasticity of the clay for the applicable stress range is

$$E_c = \frac{(1 + \nu)(1 - 2\nu)(1 + e_o)\sigma_{va}}{0.435(1 - \nu)\, C_c} = \frac{(1 + 0.42)(1 - 2 \times 0.42)(1 + 2.0)}{0.435(1 - 0.42)(0.70)} \times \left[\frac{(326 \text{ psf} + 862 \text{ psf})}{2}\right] = 2{,}292 \text{ psf} = 15.9 \text{ psi} \qquad (47)^*$$

where

E_c = drained modulus of elasticity (for a stress path along the K_o line)

ν = Poisson's ratio (drained)

σ_{va} = average of initial and final stress state applied in the field (vertical stress)

Table D2

Typical Poisson's Ratio Values of Clay for Drained Loading (Poulos 1975)

Soil Consistency	Poisson's Ratio[1]
Very Soft to Soft[2,3]	0.35 - 0.45
Firm to Stiff[2]	0.30 - 0.34
Stiff Overconsolidated Clays	0.1 - 0.29

Notes:
1. For undrained loading use 0.45.
2. For normally consolidated clays.
3. For very soft to soft clays a value of 0.40-0.45 is recommended for calculating E_c for nonlinear finite element settlement analyses of stone column improved ground; for firm to stiff use at least $\nu_c = 0.35$.

Note that the value of Poisson's ratio selected has a significant effect on the calculated value of E_c ; larger values of ν give smaller values of E_c .

5. The stone column length to diameter ratio in the soft clay is L/D = 20 ft/3.5 ft = 5.7 . The average applied pressure σ due to the embankment is σ = 1,770 psf = 12.3 psi. Interpolating from Figures 32* and 33* (a_s = 0.25) for a soft boundary condition (E_b = 12 psi), the settlement of a stone column of length L = 20 ft and diameter D = 3.5 (L/D = 5.7) is 21 in. In interpolating between figures for different S_t/L values, work in terms of settlement when the length varies. Hence, calculate the actual settlement $S_t = L\ (S_t/L)$ for each value of L/D and E_c before interpolating for settlement using a graph. The "best" settlement estimate is the average of the finite element and incremental methods: S_t = (21 in. + 31 in.)/2 = 26 in. The estimated reduction in settlement due to stone column improvement is then S_t/S = 26.0 in./45.2 = 0.575 .

Time rate of settlement

6. Determine the magnitude of primary consolidation settlement after 2 months assuming instantaneous construction (Leonards 1962). (Methods for handling construction over a finite time interval are also presented by Leonards.) The silty clay has a vertical coefficient of consolidation C_v of

0.05 ft^2/day. Based on a detailed study of the strata, the horizontal permeability is estimated to be three times the vertical permeability. Then from Equation 49*

$$C_{vr} = C_v \left(\frac{k_h}{k_v}\right) = (0.05 \text{ ft}^2/\text{day})(3) = 0.15 \text{ ft}^2/\text{day} \qquad (49)^*$$

where C_{vr} = horizontal coefficient of consolidation.

7. Assume the reduced drain diameter D' to account for smear is one-fifth the constructed stone column diameter. For an equilateral triangular stone column spacing s of 6.5 ft, the equivalent diameter D_e of the unit cell is

$$D_e = 1.05s = 1.05 \text{ (6.5 ft)} = 6.83 \text{ ft} \qquad (1)^*$$

and

$$n^* = \frac{r_e}{r_w} = \frac{D_e}{D'} = \frac{6.83 \text{ ft}}{3.5 \text{ ft}/5} = 9.76 \qquad \text{(Figure 45)}^*$$

where n^* equals ratio of unit cell radius r_e to the radius of drain r_w (stone column radius less smear zone thickness). The dimensionless vertical and horizontal time factors are then

$$T_z = \frac{C_v t}{(H/N)^2} = (0.05 \text{ ft}^2/\text{day}) \frac{(2 \times 31 \text{ days})}{(20 \text{ ft}/2)^2} = 0.031 \qquad (27)^*$$

$$T_r = \frac{C_{vr} t}{(D_e)^2} = (0.15 \text{ ft}^2/\text{day}) \frac{(2 \times 31 \text{ days})}{(6.83 \text{ ft})^2} = 0.199 \qquad (28)^*$$

where

T_z = time factor for vertical direction

C_v = coefficient of consolidation in vertical direction

t = elapsed time of consolidation

H = thickness of cohesive layer

N = number of permeable drainage surfaces at the top and/or bottom of the layer ($N = 1$ or 2)

T_r = time factor for radial drainage

D_e = equivalent diameter of unit cell

From Figure D2 (42*) the degree of consolidation in the vertical direction is $U_z = 0.12$ and from Figure D3 (43*) the degree of consolidation in the radial direction is $U_r = 0.64$. The combined degree of consolidation, Equation 25* is

$$U = 1 - (1 - U_z)(1 - U_r) = 1 - (1 - 0.12)(1 - 0.64) = 0.68 \qquad (25)*$$

where U = average degree of consolidation of the cohesive layer considering both vertical and radial drainage. An important portion of the total primary consolidation settlement occurs before 2 months and equals S_t' = 26.0 in. (0.68) = 18 in. For this example problem having stone columns, vertical drainage of the soil had little effect on the time rate of primary settlement because of the higher radial coefficient of consolidation and smaller radial drainage path to the vertical drains. For comparison, if stone columns had not been used, primary consolidation settlement would have been only 12 percent complete, with the primary settlement at the end of 2 months being only about 3 in.

Secondary compression settlement

8. Estimate the magnitude of secondary compression settlement that would be expected to occur 5 years after construction. Assume secondary compression begins at the time for 90 percent primary consolidation. Neglect the effects of vertical drainage which were shown above to be small. The radial time factor for 90 percent primary consolidation for $n^* = 9.76$ is $T_r = 0.47$ from Figure D3 (43*). From Equation 28* the time for 90 percent primary consolidation is $t = T_r(D_e)^2/C_{vr} = 0.47(6.83 \text{ ft})^2/(0.15 \text{ ft}^2/\text{day})$ = 146 days after construction. The secondary compression settlement is then

$$\Delta S = C_\alpha H \log_{10} (t_2/t_1) \qquad (30)*$$

$$\Delta S = 0.005(240 \text{ in.}) \log_{10} [5(365 \text{ days})/146 \text{ days}] = 1.3 \text{ in.}$$

where

ΔS = secondary compression of the layer

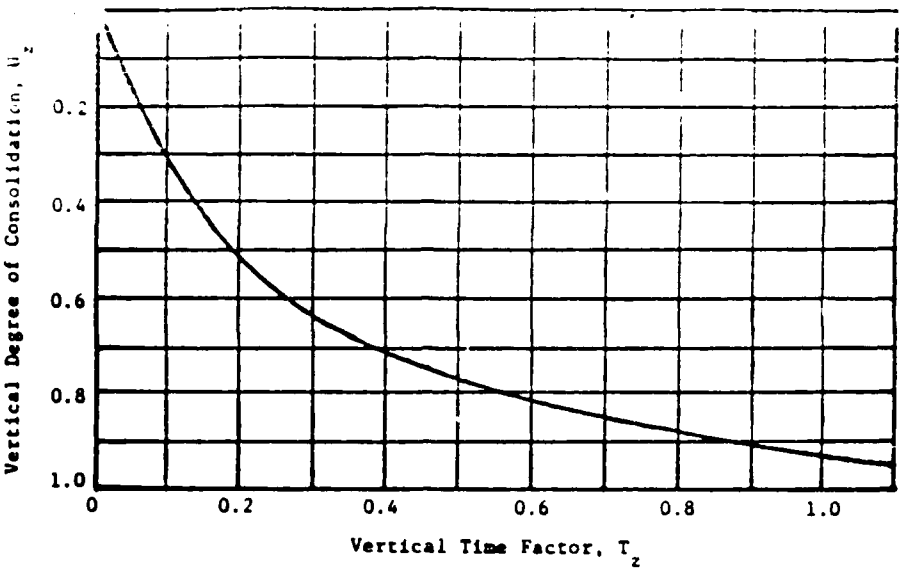

Figure D2. Degree of consolidation in vertical direction (Barksdale and Bachus 1983)

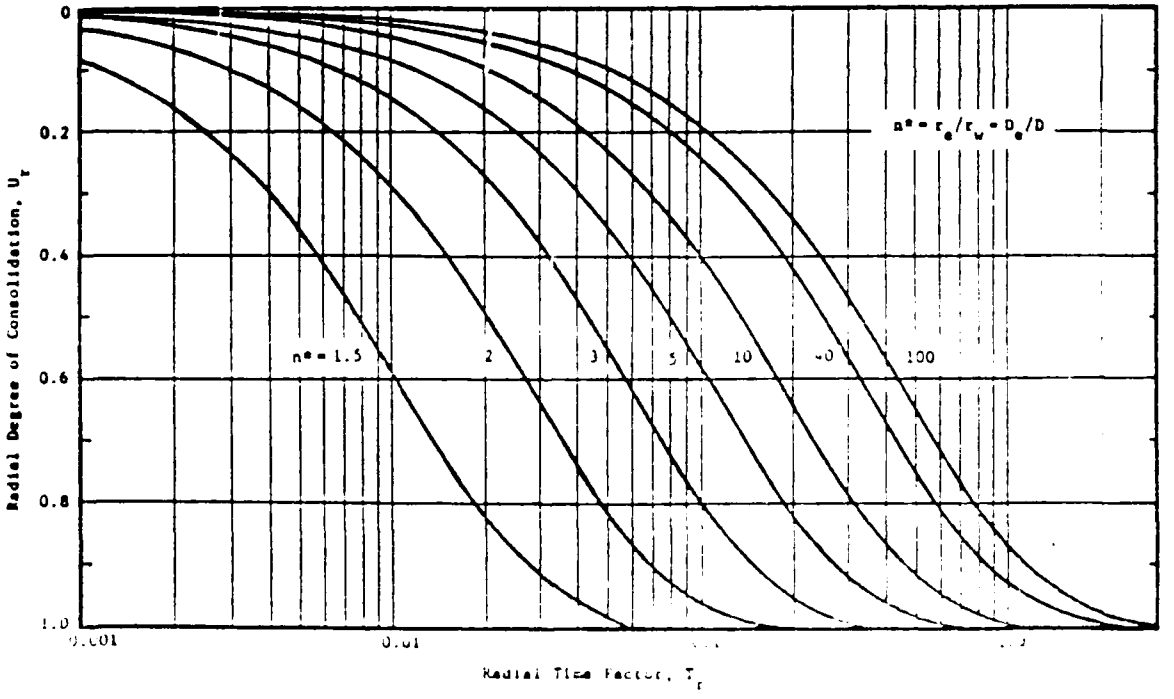

Figure D3. Degree of consolidation in radial direction (Barksdale and Bachus 1983)

C_α = physical constant evaluated by continuing a one-dimensional consolidation test past the end of primary consolidation for a suitable load increment

H = thickness of compressible layer

t_2 = time at which the value of secondary compression is desired

t_1 = time at the beginning of secondary compression; the time corresponding to 90 percent of primary consolidation is sometimes used

For the silty clay in this problem, the secondary settlement is thus relatively small compared to a primary consolidation settlement of 26.0 in. If organics had been present, secondary settlement would have been significantly greater.

Settlement Example 2

9. Settlement Example 2 illustrates how to handle, at least approximately, stress distribution in calculating settlement of stone column improved ground. Stone column improved ground is being considered as one design alternative for a slightly marginal site consisting of firm to stiff sandy silt as shown in Figure D4. The average contact stress is $\sigma = P/A = 400$ kips/(13 ft × 13 ft) = 2,367 psf. The gross area replacement ratio from Equation 3* is $a_s = A_s/A = (7.07 \text{ ft}^2)(4)/(13 \text{ ft} \times 13 \text{ ft}) = 0.167$. Now determine the initial effective stress at the center of each layer:

Layer 1: $\bar{\sigma}_o = 8$ ft (120 pcf) = 960 psf

Layer 2: $\bar{\sigma}_o = 13$ ft (120 pcf) + 4 ft (125 pcf - 62.4 pcf)
= 1,810 psf

Calculate the change in stress $\Delta\sigma_z$ at the center of each layer using as an approximation Boussinesq stress distribution theory for a square foundation and the average applied stress σ (refer to Lambe and Whitman (1969), Leonards (1962), Sowers (1979), and Winterkorn and Fang (1975) for discussion of stress distribution and for charts and tables that calculate changes in stress due to foundation loadings):

Layer 1: $z/B = \frac{5 \text{ ft}}{13 \text{ ft}} = 0.38$ (D2)

$\Delta\sigma_z = I_z \cdot \sigma = 0.82$ (2,367 psf) (D3)

$\Delta\sigma_z = 1{,}941$ psf

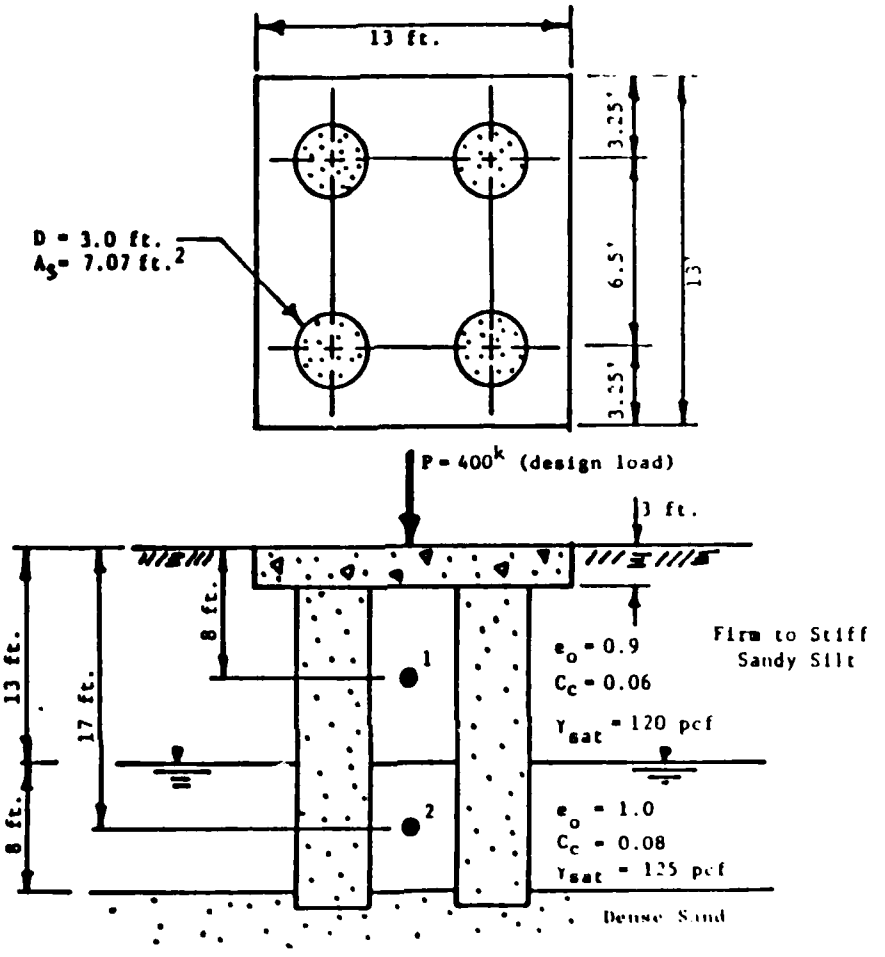

Figure D4. Settlement Example 2--Rigid Foundation Placed Over Stone Column Improved Sandy Silt

Layer 2: $z/B = \frac{14 \text{ ft}}{13 \text{ ft}} = 1.08$

$\Delta\sigma_z = I_z \cdot \sigma = 0.31 \ (2{,}367 \text{ psf})$

$\Delta\sigma_z = 734 \text{ psf}$

where

z = depth below foundation

B = foundation width

I_z = influence factor

The change in stress $\Delta\sigma_z$ calculated above is the average stress change over the unit cell.

10. Assume a stress concentration factor $n = 3$ (an n value less than 4 is used because the soil is relatively stiff compared with soft clays). The stress ratio in the sandy silt from Equation 8a* is

$$\mu_c = \frac{1}{1 + (n - 1)a_s} = \frac{1}{1 + (2.0)(0.167)} = 0.750 \qquad (8a)^*$$

The stress change in the sandy silt as an approximation can be taken to equal $\mu_c \Delta\sigma_z$ giving the following settlements from Equation 20* for layers 1 and 2:

$$S_{t1} = \left(\frac{0.06}{1 + 0.9}\right)\log_{10}\left(\frac{960 \text{ psf} + 1941 \text{ psf } (0.750)}{960 \text{ psf}}\right) (10 \text{ ft} \times 12 \text{ in.}) \qquad (20)^*$$

$$= 1.5 \text{ in.}$$

$$S_{t2} = \left(\frac{0.08}{1 + 1.0}\right)\log_{10}\left(\frac{1810 \text{ psf} + 734 \text{ psf } (0.750)}{1810 \text{ psf}}\right) (8 \text{ ft} \times 12 \text{ in.}) \qquad (20)^*$$

$$= 0.44$$

The total settlement in the sandy silt strata is about $S_t = 1.9$ in. Had stone columns not been used, the settlement would have been $S = 2.4$ in., giving $S_t/S = 1.9/2.4 = 0.79$. From Equation 22* and Figure C6 (19*), $S_t/S \cong \mu_c = 0.75$, which illustrates that $S_t/S \cong \mu_c$ is a quite useful approach for preliminary estimates of the level of reduction of settlement for various stone column designs. In the above simplified equation, the variables affecting the settlement ratio S_t/S are only a_s and n.

11. Stress distribution can also be approximately considered using the finite element design charts. To do this an average stress σ is calculated within the compressible layer and used in the chart rather than the stress actually applied at the top of the layer.

12. In Settlement Example 2, only four stone columns are used. Also, two layers of sandy silt are present which would have different coefficients of consolidation. Assume C_v (and C_{vr}) in one layer differs from C_v (and C_{vr}) in the other layer by a factor of about 2 to 5. For the resulting complex three-dimensional flow conditions, a theoretically accurate evaluation of the time rate of settlement for this problem would be a major undertaking. Such a solution would require a three-dimensional numerical analysis. As a

rough engineering approximation, however, the following simplified approach can be taken:

a. Consider for each layer radial and vertical flow separately and use Equation 25* to estimate the combined results.

b. For radial flow neglect any interaction between the two layers. Sketch in the approximate radial flow paths on a scale drawing (Figure D5). Remember that flow originates from lines of geometric symmetry and moves approximately radially to the drains.

Consider the flow to the drain shown in the upper left-hand corner of Figure D5. An examination of the flow paths on the figure show 25 percent of the flow to the stone column from quadrant a-o-b is from infinity. This means D_e for this quadrant is very large, and from Equation 28* the radial time factor $T_r = 0$. Over quadrants b-o-c and a-o-e, which together comprises another 25 percent of the drain, the flow path length varies from infinity at points b and a to short drainage paths at points c and e; this combined quadrant will only be partially

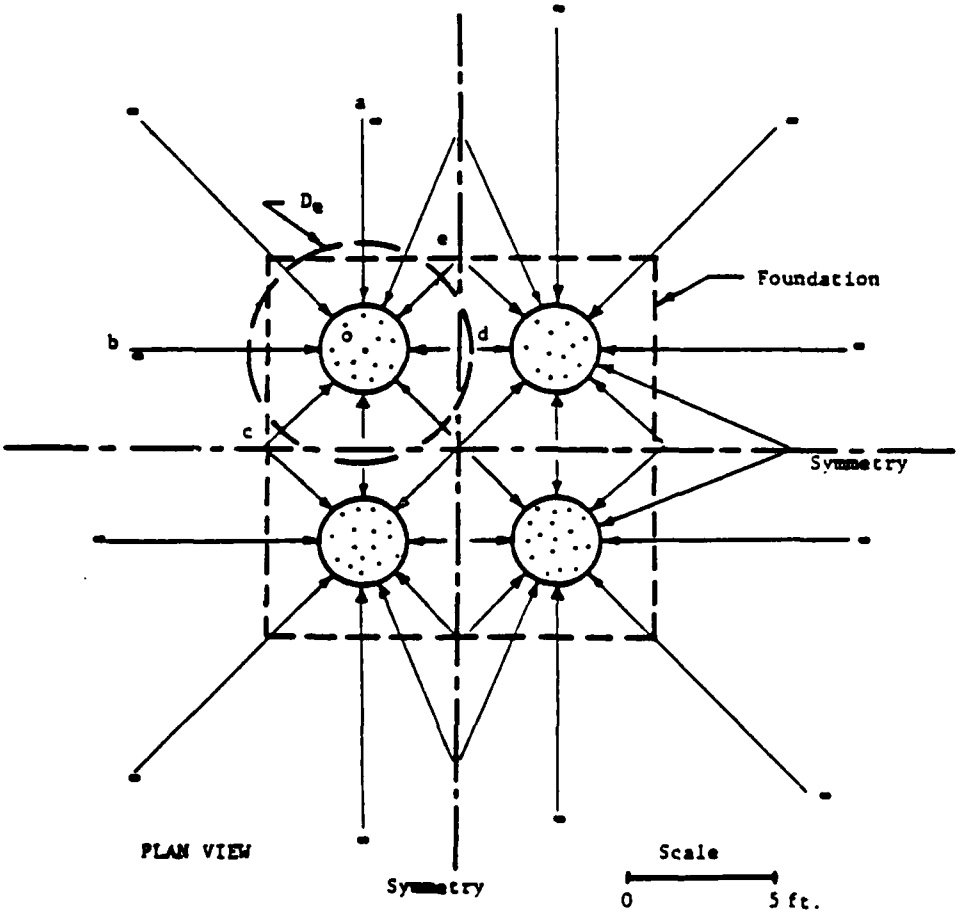

Figure D5. Approximate radial flow paths for settlement Example 2

effective in providing drainage. Finally, the area contributing flow to the drain that lies to the right and below line c-o-e has short flow paths that can be approximated by an estimated equivalent unit cell diameter $D_e \cong 7.5$ ft shown in dashed lines in the figure. As an engineering approximation for this example, estimate the time factor T_r for each layer using the appropriate value of C_{vr} and $D_e \cong 7.5$ ft. To crudely consider the D_e effectively is very large over between 25 to 50 percent of the drain, reduce the time factor by about (25 percent + 50 percent)/2 = 37.5 percent or 0.4 (multiply the calculated time factor T_r by 0.6 or use 0.5 to be a little more conservative).

To illustrate this approximate approach assume for Layer 1 $C_{vr} = 5C_v$ and $C_v = 0.2$ ft^2/day. Then at the end of 2 months the radial time factor would be estimated from Equation 28* as $T_r = C_{vr} \cdot t/D_e^2 = 5(0.2 \text{ ft}^2/\text{day})(2 \times 31 \text{ days})/(7.5 \text{ ft})^2 = 1.10$. Reducing the time factor to approximately consider partial drainage gives $T_r = 0.5 \ (1.10) = 0.55$. Assume the stone column diameter is effectively reduced by one-fifth to account for smear, giving, from Equation 29a*, $n^*_{equiv} = 7.5 \text{ ft}/(3 \text{ ft} \times 0.2) = 12.5$. Then from Figure D3 (43*) the degree of radial consolidation $U_r = 0.91$. Conservatively neglecting vertical drainage in Layer 1, the settlement after 2 months of Layer 1 is $S_{t1} \cong 1.5$ in. (0.9) = 1.35 in. As would be expected, consolidation occurs rapidly in the sandy silt.

$$r_w^* = \frac{r_e}{n^*_{equiv}} \qquad (29)^*$$

where

r_w^* = radius of drain without smear

r_e = radius of unit cell

n^*_{equiv} = radius of unit cell divided by equivalent radius of drain without smear

c. Since in this example $C_{vr} = 5\ C_v$ for Layer 1, vertical compared to radial consolidation would be relatively slow and was conservatively neglected. However, if the effect of vertical drainage on the time rate of consolidation is desired, the presence of two layers greatly complicates vertical time rate of consolidation computations. If C_v of the more permeable layer is more than 20 times C_v of the less permeable layer the following simplified approach can be used (Lambe and Whitman 1969): (1) assume consolidation occurs in two stages;

(2) in Stage 1, calculate consolidation f the more permeable layer, assuming no drainage at the interface between the two; and (3) in Stage 2, calculate consolidation in the least permeable layer, assuming drainage at the interface. If C_v of one layer is less than 20 times C_v of the other, the approximate method described in NAVFAC DM-7 (Department of the Navy 1971) can be followed or numerical methods can be used (Lambe and Whitman 1969).

d. The above methods are, of course, quite crude and should be considered "ball park" in accuracy. They do give a rational way of approaching a very complicated, three-dimensional time rate of primary consolidation problem.

REFERENCES

Barksdale, R. D., and Bachus, R. C. 1983. "Design and Construction of Stone Column," Vol I, Federal Highway Administration, Report FHWA/RD-83/026.

Department of the Navy, Naval Facilities Engineering Command. 1971. "Soil Mechanics, Foundations, and Earth Structures," NAVFAC DM-7, Washington, DC.

Lambe, T. W., and Whitman, R. V. 1969. Soil Mechanics, 1st ed., John Wiley, New York, pp 153-157.

Leonards, G. A., Editor. 1962. Foundation Engineering, 1st ed., McGraw-Hill, New York.

Poulos, H. G. 1975. "Settlement of Isolated Foundations," Proceedings, Soil Mechanics Recent Developments Symposium, University of New South Wales, Australia.

Sowers, G. F. 1979. Introductory Soil Mechanics and Foundations: Geotechnical Engineering, 4th ed., Macmillan, New York.

Winterkorn, H. F., and Fang, H. Y. 1975. Foundation Engineering Handbook, 1st ed., Van Nostrand Reinhold Co., New York, 1975, pp 128-129.

APPENDIX E: EXAMPLE STABILITY PROBLEM

1. This example illustrates how to handle the geometric and material parameters required for setting up a slope stability problem for analysis using the the Profile Method described in Chapter III, Barksdale and Bachus (1983†).

2. A 15-ft high embankment is to be placed over a soft clay as illustrated in Figure E1. Because of the low shear strength of the soft clay, use a stress concentration factor n of 2.0, and an angle of internal friction ϕ_s of the stone column of 42°. The saturated unit weight of the stone is 125 pcf. For the first trial design, use five rows of stone columns laid out as shown in Figure E1. An equilateral triangular grid will be used having a trial spacing s = 6.5 ft. The stone column diameter is estimated to be 3.5 ft, giving an area replacement ratio of

$$a_s = 0.907 \left(\frac{3.5}{6.5}\right)^2 = 0.263 \qquad (5b)^*$$

3. The plan view of the stone column grid used to improve the site is shown in Figure E1(b). As shown in the figure, stone columns replace only 26 percent of the total volume of the soft clay (i.e., $a_s = 0.263$). Further, in performing a conventional stability analysis, the materials are assumed to extend for an infinite distance in the direction of the embankment. Typically, the analysis is then performed on a 1-ft-wide slice of embankment. To use the profile method the discrete stone columns must therefore be converted into equivalent stone column strips extending along the full length of the embankment as follows:

$$A_s = \frac{\pi D^2}{4} = 3.14 \frac{(3.5 \text{ ft})^2}{4} = 9.62 \text{ ft} \qquad (E1)$$

Note: Equation, table, or figure numbers with an asterisk refer to the Federal Highway Administration stone column report (Barksdale and Bachus, 1983).

† References cited in this Appendix can be found on the last page.

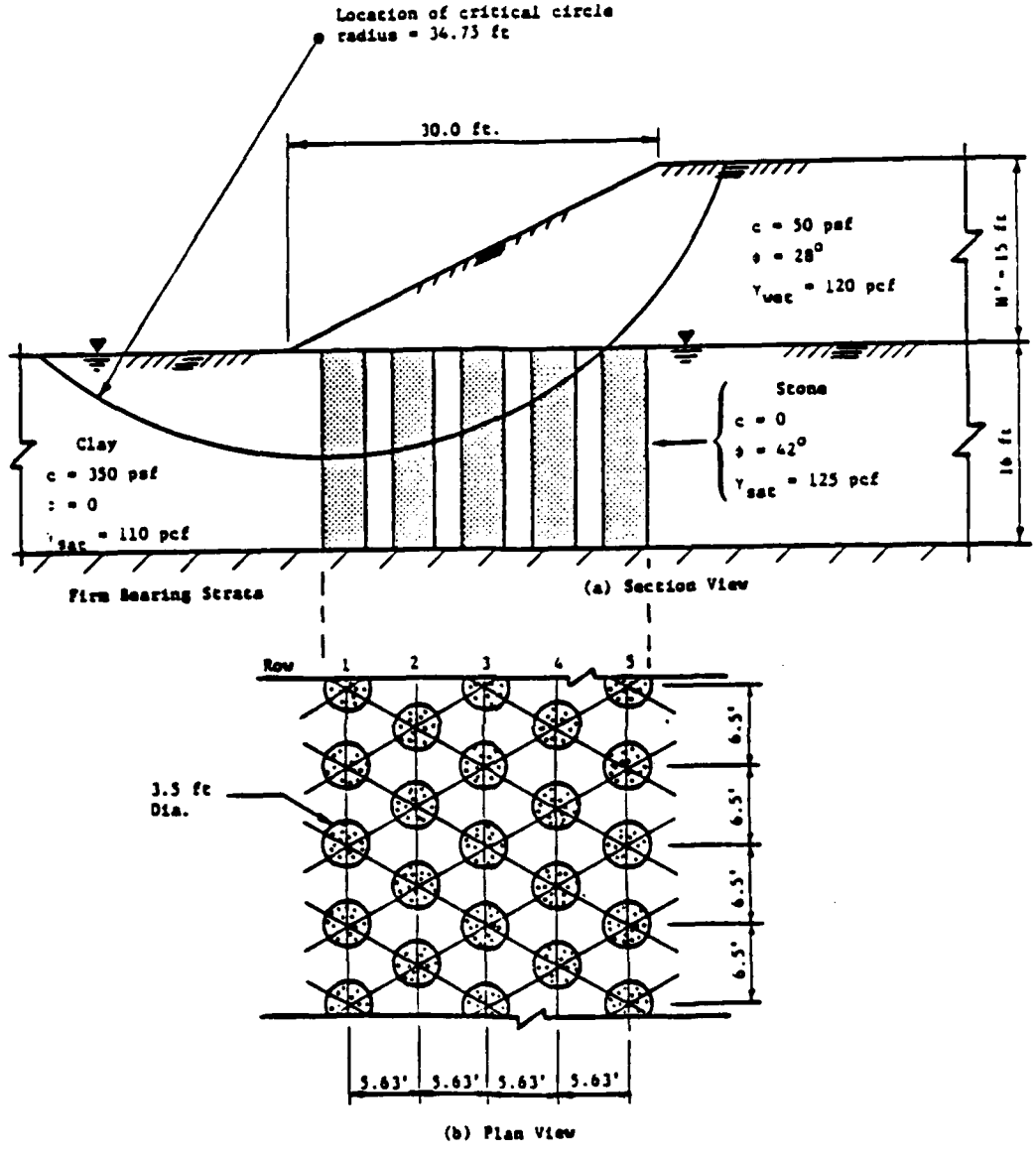

Figure E1. Stability Example Problem 1

The length tributary to each stone column in the direction of the embankment is $s = 6.5$ ft. Therefore, a solid strip having the same area and volume of stone would have a width w of

$$w = \frac{A_s}{s} = \frac{9.62 \text{ ft}^2}{6.5 \text{ ft}} = 1.48 \text{ ft} \qquad \text{(E2)}$$

The total width of the tributary area equals $A_s/(a_s s)$ = 9.62 ft^2/ (0.263 × 6.5 ft) = 5.63 ft, which is the stone column spacing 0.866s in the direction perpendicular to the embankment length.

4. Now determine the characteristics of fictitious strips (Figure E2) that must be added to handle the effect of stone column stress concentration in the stability analysis. Let the thickness $\tilde{T}$ of a fictitious strip be 0.3 ft under the full embankment. Note that in this example no stone columns are actually used under the full embankment height for the first trial. However, stone column row 5 is located so that the edge of the tributary area is just at the break in the embankment. The unit weights calculated for the full embankment height can be used for each strip, with the thickness of the strips varying from zero at the toe to 0.3 ft at the break (Figure E2). An examination of Equations 33* and 34* shows that this method gives the proper stress concentration in each strip. The thickness of the boundaries T_i of each zone is calculated in Table E1.

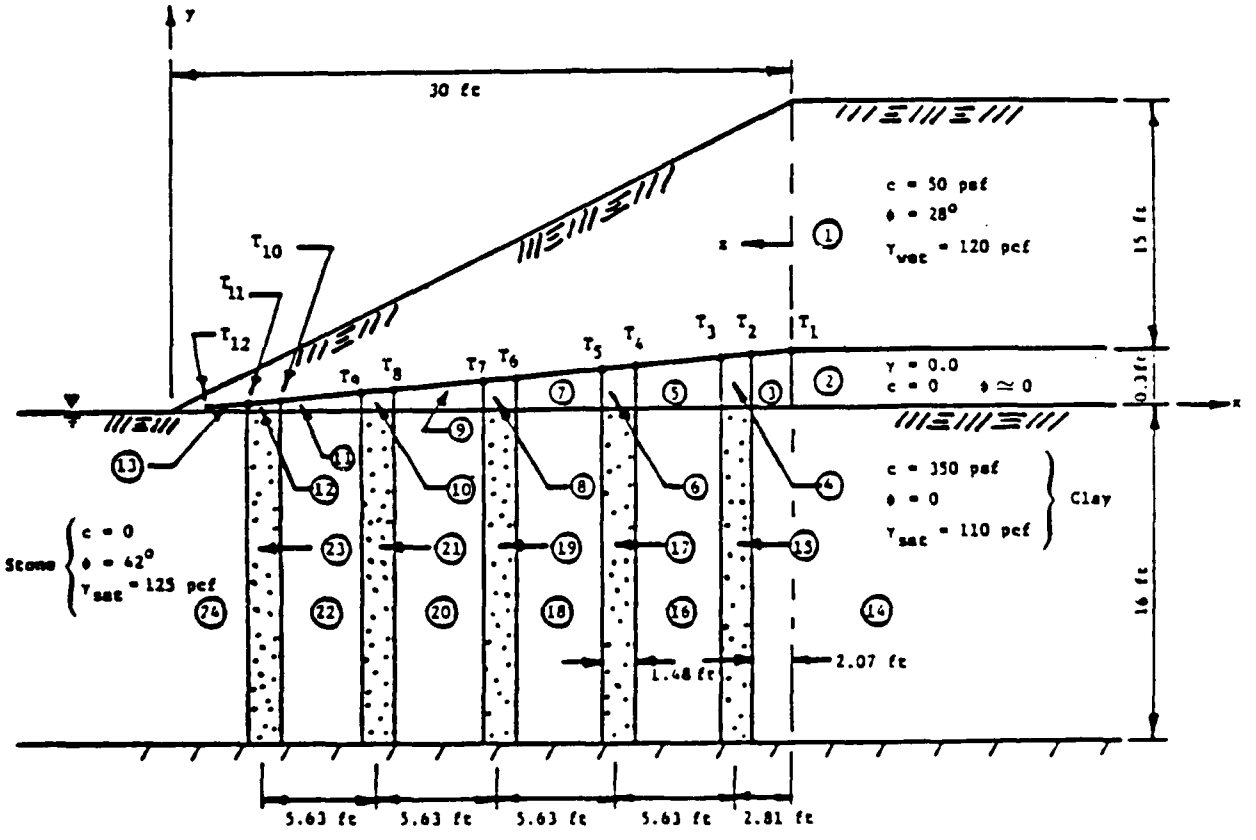

Figure E2. Zones used for computer idealization for Stability Example Problem 1

Table E1

Thickness of Fictitious Strips

Location	z ft	(30 - z) ft	Thickness, T_i, 0.01 (30 - z) ft
T_1	0	30	0.300
T_2	2.07	27.93	0.279
T_3	3.55	26.45	0.265
T_4	7.70	22.30	0.223
T_5	9.18	20.82	0.208
T_6	13.33	16.67	0.167
T_7	14.81	15.19	0.152
T_8	18.96	11.04	0.110
T_9	20.44	9.56	0.096
T_{10}	24.59	5.41	0.054
T_{11}	26.07	3.93	0.039
T_{12}	28.15	1.85	0.018

Note: T_i = Thickness of fictitious layer at location shown in Figure E2. z is defined as the horizontal distance from the break in the embankment slope to the point at which the thickness T_i is required. Then from similar triangles $T_i/(30 \text{ ft} - z) = 0.3 \text{ ft}/30 \text{ ft}$.

5. The unit weights to use in the fictitious strips are calculated as follows:

$$\mu_s = \frac{n}{[1 + (n - 1)\, a_s]} = \frac{2.0}{[1 + (0.263)]} = 1.58 \qquad (8b)^*$$

$$\mu_c = \frac{1}{[1 + (n - 1)\, a_s]} = \frac{1.0}{[1 + (0.263)]} = 0.792 \qquad (8b)^*$$

6. The correct unit weight to use above each stone column in the fictitious strip is

$$\gamma_f^s = (\mu_s - 1)\gamma_1 H'/T = \frac{(1.58 - 1)(120 \text{ pcf})(15 \text{ ft})}{0.3 \text{ ft}} \qquad (33)^*$$

$$= 3{,}480 \text{ pcf}$$

and the unit weight to use above the soil in each fictitious strip is

$$\gamma_f^c = (\mu_c - 1)\gamma_1 H'/T = \frac{(0.792 - 1)(120 \text{ pcf})(15 \text{ ft})}{0.3 \text{ ft}} \quad (34)^*$$
$$= -1{,}248 \text{ pcf}$$

where

γ_1 = unit weight of embankment

H' = height of embankment

7. Material properties and zones are as follows (refer to Figure E2):

Zone 1: $\gamma_w = 120$ pcf, $c = 50$ psf, $\phi = 28°$

Zone 2: $\gamma_w = 0$, $c = 0$, $\phi = 0$

Zones 3, 5, 7, 9, 11, 13: $\gamma = -1{,}248$ pcf, $\phi = 0$, $c = 0$

Zones 4, 6, 8, 10, 12: $\gamma = +3{,}480$ pcf, $\phi = 0$, $c = 0$

Zones 14, 16, 18, 20, 22, 24: $\gamma_{sat} = 110$ pcf, $\phi = 0$, $c = 350$ psf

Zones 15, 17, 19, 21, 23: $\gamma_{sat} = 125$ pcf, $\phi = 42°$, $c = 0$

8. The calculated safety factor of the slope is shown in the table below for the following conditions: (a) no improvement with stone columns, (b) the stone column improvement shown in Figure E1 using a stress concentration factor $n = 1$, and (c) the same level of improvement with $n = 2.0$ (the critical circle for this condition is shown in Figure E1). A simplified Bishop analysis was performed using the GTICES Lease II computer program prepared by A. W. Dawson (1972).

Table E2

Safety Factors

Case	n	Coordinate[1] x ft	Coordinate[1] y ft	R ft	S.F.	Comment
1. No S.C.[2]	-	14.20	27.00	43.00	1.07	Base Failure
2. S.C.	1	2.90	26.00	42.00	1.38	Base Failure
3. S.C.	2.0	2.90	26.00	34.75	1.65	See Figure E1

Notes: 1. Coordinates of critical circle (refer to Figure E1 for location of x and y axles).

2. Notation: S.C. = stone column; S.F. = Safety factor; R = radius of critical circle.

REFERENCES

Barksdale, R. D., and Bachus, R. C. 1983. "Design and Construction of Stone Columns," Vol I, Federal Highway Administration, Report FHWA/RD-83/026.

Dawson, A. W. 1972. "LEASE II - A Computerized System for the Analysis of Slope Stability," thesis presented to the Massachusetts Institute of Technology in partial fulfillment of the requirements for the degree of Bachelor of Science in Civil Engineering, Boston.

APPENDIX F: EXAMPLE PROBLEM OF PORE PRESSURE DISSIPATION DURING AN EARTHQUAKE

1. Stone columns approximately 30 ft in length are to be used in loose sands to (a) densify the sand, (b) provide additional lateral shear strength, and (c) dissipate pore pressures generated during an earthquake. The site conditions consist of alluvial, generally loose, fine-to-medium-grained sands interbedded with silt and clay layers and lenses. The maximum triangular pattern stone column spacing s is required to prevent liquefaction from occurring within the sand layers during a design earthquake.

2. An equilateral triangular pattern of stone columns is to be employed. The stone columns will be constructed using a processed river gravel having a maximum size of 1.5 in., and a minimum size of 0.375 to 0.5 in. The completed diameter of the stone columns is estimated to be 3.0 ft. The sands have a horizontal permeability of about 0.007 ft/min, and a coefficient of compressibility m_{v3} of 2.5×10^{-6} ft^2/lb. Both permeability and compressibility were estimated for conditions after stone column construction. The characteristics of the earthquake as determined from a separate detailed earthquake analysis are as follows:

$$\frac{N_{eq}}{N_{\ell}} = 1.5 \tag{F1}$$

$$t_d = 0.5 \text{ min} \tag{F2}$$

where

N_{eq} = number of uniform stress cycles equivalent to earthquake

N_{ℓ} = number of cycles to liquefaction

t_d = time over which the N_{eq} uniform stress cycles of the earthquake are applied

3. The stone columns are to be constructed using the pull-down process. The jets on the outside of the vibroflot (casing) and the horizontal vibrator will both be operated during construction. Use of this construction technique will prevent sand from being deposited within the open-graded stone backfill. Although the effects of smear should be relatively small using this technique, some smear in the sand may result due to dragging of soil from the cohesive layers. Therefore, assume the effective stone column diameter is one-half of the actual diameter of 3 ft.

4. The permeability of the stone column backfill material as measured in the laboratory is 35 ft/min. Hence the ratio of the vertical stone column drain to the in situ sand permeability is 35 ft/min/0.007 ft/min = 5,000 . This value is considerably greater than the ratio of 200 indicated by Seed and Booker (1976)† for water to readily move vertically through the stone column during an earthquake.

5. To determine the required stone column spacing, first calculate the dimensionless time factor

$$T_{ad} = \frac{4k_r t_d}{\gamma_w m_{v3} D^2} \quad \frac{4(0.007 \text{ ft/min})\ (0.50 \text{ min})}{(62.4 \text{ lb/ft}^3)\ (2.5 \times 10^{-6} \text{ ft}^2/\text{lb})\ (1.5 \text{ ft})^2} \qquad \text{(F3)}$$

$$T_{ad} = 39.9$$

where

k_r = horizontal permeability of the sand stratum

γ_w = unit weight of water

m_{v3} = coefficient of compressibility

D = diameter of the stone column

Note that the actual stone column diameter of 3 ft has been reduced by one-half in the above equation to crudely account for possible smear.

6. To be conservative use a safety factor of 1.5 with respect to the greatest pore pressure ratio in the sand, i.e., let the greatest allowable value of the pore pressure ratio $r_g = 1/SF = 1.0/1.5 = 0.67$. Since $N_{eq}/N_\ell = 1.5$, interpolation using Figures 3, 4, and 5 (see main text) is required as follows:

Figure	N_{eq}/N	Required D/D_e
3	1	0.11
4	2	0.19
5	3	0.24

By interpolating from a plot of the above data for $N_{eq}/N_\ell = 1.5$, the required ratio $D/D_e = 0.16$. Hence $D_e = D/0.16 = 1.5 \text{ ft}/0.16 = 9.4$. Since the stone column spacing $s = D_e/1.05$, then $s = 9.4 \text{ ft}/1.05 = 8.95 \text{ ft}$. A

† References cited in this Appendix can be found on the last page.

9-ft triangular spacing should therefore provide effective lateral dissipation of excess pore pressure during the design earthquake. Of course, all other pertinent factors such as required sand relative density, settlement, and shear should be considered in selecting a final stone column spacing.

REFERENCE

Seed, H. B., and Booker, T. R. 1976. "Stabilization of Potentially Liquefiable Sand Deposits," Report EERC 76-10, University of California, Berkeley, Earthquake Engineering Research Center, Berkeley, Calif.

APPENDIX G: NOTATION*

a_s	Area replacement ratio, A_s/A
A	Total area within the unit cell
A_s	Stone column area
B	Foundation width
c	Cohesion of soil
C_c	Virgin compression index of cohesive soil from one-dimensional consolidation test
C_α	Coefficient of secondary compression, $C_\alpha = \Delta H/\left[H \log_{10} (t_2/t_1)\right]$
C_v	Coefficient of consolidation in vertical direction (Equation 27)
C_{vr}	Coefficient of consolidation in radial direction (Equation 28)
D	Constructed diameter of stone column (Figures 13 and 14)
D_e	Equivalent diameter of unit cell (Equations 1 and 2)
e_o	Initial void ratio of cohesive soil
E	Modulus of elasticity
E_b	Modulus of elasticity of thin boundary around the unit cell used in nonlinear finite element analysis
E_c	Modulus of elasticity of soil within the unit cell
E_s	Modulus of elasticity of the stone column
F	Shear force on upper failure surface in stone column undergoing local bearing failure (Appendix B)
F'_c, F'_q	Vesic cavity expansion factors (Figure 16)
h	Depth of fill above the stone column
H	Vertical height (or increment) of stone column treated ground over which settlements are calculated
H'	Height of embankment in stability analysis (Figure 46)

Note: Equation, table, or figure numbers refer to the Federal Highway Administration stone column report (Barksdale and Bachus, 1983).

* References cited in this Appendix can be found in the References at the end of the main text.

I_r Rigidity index used in Vesic cavity expansion theory (Equation 13)

k Horizontal permeability of the sand stratum

k_r Permeability of soil in radial direction (Figure 45)

k_s Permeability of smear zone in radial direction (Figure 45)

k_v Permeability of soil in vertical direction

K_o Coefficient of at-rest earth pressure

L Length of stone column

m_{v3} Coefficient of compressibility

n Stress concentration factor, σ_s/σ_c (Figure 14)

n^* Ratio of the unit cell radius to the radius of the drain (stone column radius less smear zone thickness), $n^* = r_e/r_w$ (Figure 43)

n^*_{equiv} Equivalent value of n^* for a drain without smear, $n^*_{eq} = r_e/r^*_w$ (Figure 44)

N Number of drainage surfaces at the top and bottom of the layer ($N = 1$ or 2); also normal force on lower failure surface in stone column undergoing local bearing failure (Appendix B)

N_c Ultimate bearing capacity factor of stone column (Equation 50)

N_{eq} Number of uniform stress cycles equivalent to earthquake

N_ℓ Number of cycles to liquefaction

P_H Ultimate lateral resistance of clay acting on critical wedge for a local bearing failure of stone column (Appendix B)

P_{ult} Ultimate loading that can be applied over the unit cell area

q Mean isotropic stress, $q = (\sigma_2 + \sigma_2 + \sigma_3)/3$

q_{ult} Ultimate bearing capacity

$\tilde{q}_{ult}$ Ultimate bearing capacity of stone column

r_e Radius of the unit cell (Figure 45)

r_g Greatest pore pressure ratio

$\bar{r}_g$ Greatest average pore pressure ratio

r_s Radius of smear zone (Figure 45)

r_w Radius of the drain usually taken as the radius of the stone column less the thickness of the smear zone (Figure 45)

r_w^* Radius of equivalent drain without smear (Figure 45)

R Radius of the stone column

s Center to center spacing of stone columns (Figure 13)

s* Ratio of the radius of smear zone to radius of the drain, $s^* = r_s/r_w$ (Figure 44)

S Settlement of unimproved ground

S_t Settlement occurring in an increment H of stone column treated ground

S_t' Primary consolidation settlement at time t

S_1 Settlement of a single stone column (Figure 50)

t Time

t_d Time over which the N_{eq} uniform stress cycles of the earthquake are applied

T Shear force on lower failure surface in stone column undergoing local bearing failure (Appendix B)

$\tilde{T}$ Assumed thickness of fictitious strip of soil used to obtain proper stress concentration in a computer stability analysis (Figure 46)

T_r Time factor for radial drainage, $T_r = C_{vr}\, t/(D_e)^2$ (Figure 43)

T_z Time factor for vertical drainage, $T_z = C_v t/(H/N)^2$ (Figure 42)

T_{ad} Dimensionless time factor

u Induced pore pressure

U Average degree of consolidation considering both vertical and radial drainage, $U = 1 - (1 - U_z)(1 - U_r)$

U_r Average degree of consolidation in radial (horizontal) direction (Figure 43)

U_z Average degree of consolidation in vertical direction (Figure 42)

w Width of equivalent, continuous stone strip used in a stability analysis $w = A_s/s$ (Figure 46)

$\tilde{W}_N$ Effective normal force exerted on upper failure wedge-local bearing failure (Appendix B)

W_s Effective weight of stone in failure wedge-local bearing failure of stone column (Appendix B)

$\bar{W}_v$ Effective vertical force exerted on the circular arc failure surface or the upper surface of the failure wedge for local bearing failure (Appendix B)

z Depth below ground surface

z_o Depth of circular arc failure below top of stone

α Inclination of lower failure surface in a stone column undergoing a local bearing failure (Appendix B)

α_1 A parameter characterizing the shape of the pore pressure generation curve

β Inclination of shear surface with respect to the horizontal

γ_c Saturated (wet) unit weight of cohesive soil

γ_f^c Weight of fictitious soil strip for use in computer stability analysis, $\gamma_f^c = (\mu_c - 1)\gamma_1 H/\tilde{T}$ (Figure 46)

γ_f^s Weight of fictitious soil strip for use in computer stability analysis, $\gamma_f^s = (\mu_s - 1)\gamma_1 H/\tilde{T}$ (Figure 46)

γ_s Saturated (wet) unit weight of stone column

$\bar{\gamma}_s$ Bouyant unit weight of stone in failure wedge-local bearing failure

γ_w Unit weight of water

γ_{avg} Average unit weight of material within unit cell

γ_1 Unit weight of embankment in stability analysis (Figure 46)

η Reduction factor for local bearing failure of a stone column (Appendix B)

μ Reduction factor to apply to measured field vane shear strengths (Figure 73)

μ_c Ratio of stress in cohesive soil to average stress, $\mu_c = \sigma_c = \sigma_c/\sigma$ (Equation 8a)

μ_s Ratio of stress in stone column to average stress, $\mu_s = \sigma_s/\sigma$ (Equation 8b)

ν Poisson's ratio

ν_c Poisson's ratio of soil

ν_s Poisson's ratio of stone column

σ Average stress acting over the unit cell area due to the applied loading (Figure 14); stress distribution should be considered with depth where important (Figure 40)

σ_c Average stress acting over the soil in the unit cell (Figure 14)

σ_s Average stress acting over the stone column (Figure 14)

$\bar{\sigma}_o$ Initial effective stress in cohesive soil before stone column construction

σ_{va} Average of initial and final stress state applied to the cohesive soil; σ_{va} is used in Equation 47 to calculate E for consolidation test results

σ_1 Major principal stress

σ_3 Minor principal stress

τ_c Shear strength in cohesive soil on failure surface in a stability analysis

τ_s Shear strength in stone on failure surface in a stability analysis

τ_{eq} Earthquake equivalent uniform stress

ϕ_c Angle of internal friction of soil

ϕ_s Angle of internal friction of stone column

Ψ tan α - tan β (Equation 56)

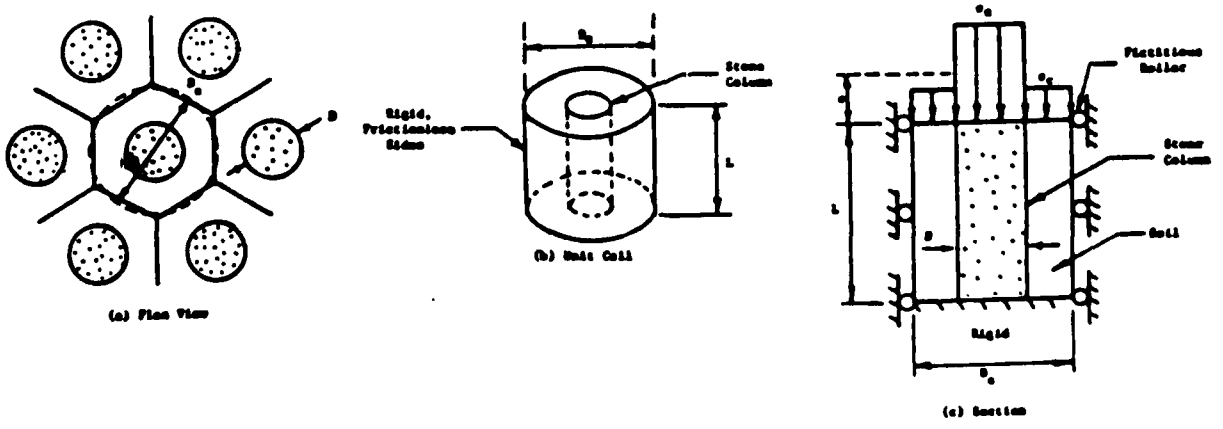

Figure G1. Unit cell idealization

END

DATE

FILMED

5-88

DTIC